Politecnico di Milano

School of Industrial and Information Engineering
Department of Aerospace Science and Technology (DAER)
Master of Science in SPACE ENGINEERING
Academic Year 2019 - 2020

ASTERIA:

Integration of Risk Collision Management in Autonomous Orbit Control

Master Thesis

STUDENT:
Chiara Maria Paola Rusconi
ID NUMBER: 899854

SUPERVISORS:
CNES - **Jérôme Thomassin**
ISAE Supaero - **Prof. David Mimoun**
Politecnico di Milano - **Prof. Camilla Colombo**

ASTERIA

Integration of Risk Collision Management in Autonomous Orbit Control

A te Pietro, per ringraziarti di aver iniziato questo percorso
con noi e per il sorriso che so ci stai rivolgendo anche oggi.

Acknowledgements

First, I would like to thank my supervisor Jérôme Thomassin, who guided and followed me in this internship by always being open for sharing ideas and supporting me in this beautiful experience. A second thank goes to Maxime Echoard, Géraldine Constant-Filaire and the whole team of DSO/DVO/MS for welcoming me during these six months at CNES. I would equally like to thank my supervisor Professor Camilla Colombo, not only for her support in this specific experience but also for transmitting me her passion for the orbital mechanics in the courses at Politecnico. My special thanks are extended to the interns' team at CNES, to Yohan, Guido, Dexter, Linh, Marcos, Jérémy, Massyl, who enriched my internship with a delightful conviviality component. Sharing common passions and spending good times with you have made more pleasant my days spent at CNES.

Un riconoscimento sincero va ai miei amici di Tolosa: Federico, Caterina, Vincenzo, Federico, Michael, My-Loan, Jacques e tutti gli altri che hanno rappresentato per me una seconda famiglia oltre confine. E tra questi, voglio rivolgere un ringraziamento speciale a Tommaso, per tutti i momenti di serenità passati assieme e, ancor più, per quelli in cui siamo stati un conforto uno per l'altra. Un grazie importante è per te, Rebecca, compagna tra i banchi e amica al di fuori dell'università. Sono contenta di aver potuto concludere questo percorso con te e sono sicura che dovunque ti porterà il tuo futuro non smetterai mai di brillare.

Sarò sempre grata ai miei amici di Milano: Giulia, Elena, Luca, Marta, Giovanni, Andrea, Sebastiano, Sergio, Virtudes, Demetrio, Cristina. Siete il motivo per cui ancora oggi riguardo agli anni passati a Milano con estrema nostalgia. E mi ricordate ogni giorno l'importanza di avere accanto a sé delle persone care nei momenti di difficoltà. Un grazie particolare lo rivolgo ad Alfonso: nonostante le centinaia di chilometri di distanza, sei sempre riuscito a trovare il modo di dimostrarmi che amico fedele tu sia. Un ringraziamento molto speciale va ad Umberto, che nel corso di questi anni è stato per me compagno di università e di momenti fantastici di vita. Grazie per essere stato sempre al mio fianco, spronandomi ogni giorno con affetto. Spero tu possa riconoscere in te stesso quel grande potenziale che hai sempre visto in me.

Un grazie ai miei zii, ai miei cugini e a tutti i miei parenti. Sono estremamente grata di appartenere a una famiglia in cui il supporto reciproco è una costante fondamentale. Voglio ringraziare le mie splendide sorelle Alessandra e Francesca, per rappresentare per

me il più naturale e spontaneo degli affetti. Nonostante non siate qui con me oggi, vi posso immaginare al mio fianco, cercando di trasmettermi serenità e coraggio, ma lasciando trapelare quel poco di sana agitazione che porta con sé emozione e solidarietà. Infine, ringrazio immensamente i miei genitori. Grazie per avermi supportata lungo questo percorso universitario e, più in generale, in tutti questi anni. Anche in questa occasione vi sento qui vicini a me, dove siete sempre stati, nonostante i chilometri di distanza. E rivolgendovi queste parole, voglio essere io, oggi, ad esprimervi il mio orgoglio nei vostri confronti, per essere stati un esempio da seguire, per aver creduto in me e nelle mie capacità, e per essere, da sempre, i miei più grandi sostenitori.

Abstract

Station-Keeping operations are essential in a satellite mission for counteracting the trajectory deviations caused by perturbing forces. Despite the advantages in adopting an embedded solution, its implementation is complicated by the emergence of a parallel need: the collision avoidance management. In a spatial environment which is always more crowded, a proper coupling between the station keeping and the management of the space objects in the vicinity of the satellite is necessary. However, the collision avoidance strategies demand an accurate knowledge of the satellite trajectory which contrasts with the advisable reactivity of an on-board control system.
The Centre National d'Etudes Spatial (CNES) developed embedded solutions for both the orbital control and the collision risk management. The aim is to strengthen the satellite autonomy, to manage the collisions issue and to further reduce the on-ground operations load at once. This thesis work has contributed to this ambitious project by designing ASTERIA: an on-board solution which merges the two subsystems in an embedded controller able to autonomously maintain the orbit and manage the collision risk. The original functioning of the two subsystems is initially presented. In a second time the introduced upgrades are described. They have been conceived for both allowing the merge and amplifying the initial functionalities. Finally, the analysis of a strategy for the construction of a collision avoidance manoeuvre is presented. The strategy is designed to strengthen the system autonomy, by making the satellite able to detect a future collision and react for avoiding it while, as well, ensuring the mission.

Keywords: *Autonomous Orbit Control, Station-Keeping, LEO, Collision Risk, Debris, Collision Avoidance Strategy , OPS-SAT*

Sommario

Nella fase operativa di un satellite, le attività di station-keeping sono essenziali per limitare gli effetti di perturbazioni sull'orbita. Nonostante i vantaggi di una soluzione a bordo, la sua implementazione è complicata dalla presenza di una necessità parallela: la gestion dei rischi di collisione. In un contesto spaziale sempre più popolato, un'appropriata integrazione tra station-keeping e la gestione dei corpi orbitanti nelle vicinanze del satellite è necessaria. Tuttavia, le strategie di prevenzione di collisione, gestite da potenti calcolatori a terra, richiedono un livello di accuratezza nella conoscenza della traiettoria del satellite che si oppone alla reattività che caratterizza un sistema di controllo autonomo efficiente. Per fare fronte a questa questione, il Centro Nazionale di Studi Spaziali Francese (CNES) ha concepito due sistemi a bordo, finalizzati rispettivamente a garantire un corretto station-keeping e gestire il calcolo di rischio di collisioni. Lo scopo è quello di incrementare il livello di autonomia del satellite, riducendo il volume di operazioni richiesto alle stazioni al suolo. Questa tesi ha contribuito allo sviluppo di questo progetto, nella realizzazione di ASTERIA: un sistema integrale a bordo in grado di proporre un piano di manovre di mantenimento orbitale e di validarlo attraverso un controllo sui rischi di collisione. Inizialmente, il funzionamento originale dei due singoli sistemi é presentato. In seguito, l'attenzione si focalizza sulle modifiche apportate volte, sia a realizzare la fusione dei due sottosistemi in ASERIA, sia ad ampliarne le funzionalità. Infine, lo studio si concentra sulla concezione di un piano di prevenzione da collisioni. Tale strategia è volta a incrementare l'autonomia del sistema di controllo, rendendo il satellite non solo in grado di rilevare potenziali rischi, ma anche di mettere in atto un piano di manovre che permetta di evitare la collisione e garantire, in seguito, il proseguimento della missione.

***Keywords**: Controllo Orbitale Autonomo, Station -Keeping, LEO, Calcolo di Rischio di Collisione, Detriti Spaziali , Strategia di Prevenzione da Collisioni, OPS-SAT*

Contents

List of Figures

List of Tables

Acronyms

AN	Ascending Node
ANGELS	Argos Neo on a Generic Economical and Light Satellite
AOC	Autonomous Orbit Control
AOCS	Attitude and Orbit Control System
AOL	Argument Of Latitude
ASTERIA	Autonomous Station-keeping Technology with Embedded collision RIsk Avoidance system
CAM	Collision Avoidance Manoeuvre
CDM	Conjunction Data Message
CROCO	Collision Risk On board COmputation
FH	Frozen Horizon
FSF	Frozen Semi Frozen
GEO	Geo Stationary Orbit
GNSS	Global Navigation Satellite System
GPS	Global Positionning System
IP	In Plane
LEO	Low-Earth Orbit
LQR	Linear Quadratic Regulator
LT	Local Time
MC	Monte Carlo
OD	Orbit Determination
OOP	Out Of Plane
SFH	Semi Frozen Horizon
SI	Intarnational System of Units

SK	Station Keeping
SMA	Semi Major Axis
SSO	Sun Synchronous Orbit
TAI	International Atomic Time
TCA	Time of Closest Approach
Thsld	Threshold
UTC	Coordinated Universal Time
wrt	with reference to

Symbols

a	semi-major axis
α	argument of latitude
ΔN	normal deviation
ΔT	tangential deviation
ΔW	out-of-plane deviation
e	eccentricity
η	manoeuvre efficiency
e_X, e_Y	eccentriity components
F	thrust
G	universal gravitational contant
$\vec{h}$	angular momentum
i	inclination
M	mean anomaly
μ	Earth standard gravitaion parameter
n	orbital angular speed
ν	true anomaly
ω	argument of pergee
Ω	right ascension of the ascending node
p	primary object
P_{coll}	probability of collision
π	numerical value of pi

$\vec{r}$	position vector
s	secondary object
σ	standard deviation
t	time variable
T_0	orbital period
$\vec{v}$	velocity vector
V	avarage linear speed
$\vec{X}$	state vector
ζ	orbital elements vector

Chapter 1

Introduction

1.1 Project background

1.1.1 Autonomous orbital control system

The scientific community has showed, since the beginning of the space investigation, a growing interest in making satellites autonomous in order to both increase their independency in view of deep space exploration missions and to reduce the on-ground operations load. In this perspective, important goals have been achieved with the introduction of autonomous navigation systems and on-board attitude controller. The integration of the Autonomous Orbital Control (AOC) represents a new milestone by providing both increased mission performances and significant operations cost reduction. For this reason, the space scientific community has been investigating its design and implementation since the 90's. In 1992, Maute proposed a method which exploits star trackers and solar detectors for measuring the angles formed between the satellite and the Sun, the Polar Star and the Earth to determine its state vector and the required Station-Keeping (SK) manoeuvres [20]. In 1994 Chan and Bernstein analysed the possibility of exploiting the Global Positioning System (GPS) receivers for on-board station-keeping on Geostationary Orbits (GEO) [4]. In the same years the NASA was investigating the possibility of producing an autonomous control system in view of future interplanetary missions pointing to Mars [22]. Since the beginning of the 21st century the Microcosm, Inc [33] has showed its interest in the conception of an autonomous control system in collaboration with the NASA for reducing the operational costs of satellite missions. This implementation couples an on-board orbit determination obtained by means of a numerical propagation and GPS measurements over an extended period. The controller analyses the deviation of the orbit elements (in particular the period of the orbit and the in-track phase) from their expected values and generates thruster firing commands for correcting the orbit. Both

De Florio [10] and Pervez [35] study controllers solutions based on a feedback system. The one proposed by Pervez, in particular, suggests the use of a multivariate feedback regulator based on a Linear Quadratic Regulator (LQR) conceived for minimising both the control error on the satellite state and the control effort. This solution shows good performances, especially because it does not need to estimate non-Keplerian forces by adopting an analytical model, but it computes the orbit and the needed manoeuvres punctually.
However, one drawback of these solutions is that they do not allow long-term prediction of the satellite dynamic. Moreover, they do not consider the issue of the integration of an autonomous controller with the parallel operations performed by the collision risk management. The space debris avoidance strategy needs an accurate knowledge of the satellite orbit in addition to a long computational time. These requirements can not be achieved with standard on-board orbit control.
The AOC developed by CNES [31] does propose a solution to these limitations. Its advantages are several:

1. it allows to handle an extended horizon of analysis.
2. it has been conceived for reducing the fuel consumption by exploiting the natural orbit evolution under the effect of the perturbating forces.
3. it is functional with both a chemical and a low thrust propulsion system.
4. it can perform different kinds of manoeuvres according to the need: in-plane, out-of-plane control or both of them at once (mixed-manoeuvre).
5. it significantly reduces the total operation costs. It has been estimated that for Low Earth Orbit missions the AOC implementation would represent a net saving in total annual operations cost in the order of $10 - 20\%$ [7].
6. it has been conceived for being compatible with the space collisions risk management thanks to an higher level of predictability [7].

The later point, in particular, is what makes the AOC innovative in comparison with other competitors. Indeed, even a completely autonomous system which shows to have very high performances in orbital covering loses in efficiency if the ground centre is asked to constantly check for possible collision with the satellite neighbourhood. This issue and others presented in the next paragraph led the CNES to develop an on-board collision management system.

1.1.2 Space collision management

Space pollution in Earth vicinity represents a significant issue for both the satellites which are currently orbiting around our planet and the future launches. The situation becomes more critical when considering the narrow altitude bands associated with communication

satellite constellations in Low Earth Orbits and Geostationary Earth Orbits [16].
The space artificial population is composed by:

- operative satellites;
- inoperative satellites;
- spatial debris generated as a result of explosions, collisions or stage separations. [1]

In this complex new reality, a space legislation for detecting and managing the space objects is then essential. This led the NASA to introduce the following five norms [30]:

1. Limiting the generation of debris associated with normal space operations.
2. Depleting on-board energy sources after completion of mission for extinguishing the risk of on-orbit explosions.
3. Limiting orbit lifetime after mission completion to 25 years or manoeuvring to a disposal orbit.
4. Limiting the consequences of impact with existing orbital debris or meteoroids.
5. Limiting the risk from space system components surviving re-entry as a result of post mission disposal.

Despite the introduction of this regulation, in the following years, some events have significantly increased the number of spatial debris. In 2007 the China has destroyed its satellite *FengYun 1C* by causing an increase of 25% of the global known debris population [3]. In 2009 the first accidental space collision occurred between the American satellite *Iridium 33* and the soviet one *Kosmos 2251* [23]. The impact generated more than 2300 debris. To avoid other accidents in an always more crowded environment, the space community was led to the development of tools for cataloguing all the in-space objects and for predicting space collisions [13], [18]. For this purpose the defence department of the United States of America created the *Space Surveillance Network* which collects information about all the space objects with a diameter greater than 5 cm in LEO and greater than 1 m in GEO [32]. Further developments led to a second-generation tracker: *Space Fence*, managed by the US Air force [2]. Similarly the ESA constantly cooperates with specific centres for the detection of space bodies. This is the case of, for example, the *Tracking and Imaging Radar* operated by Germany's Fraunhofer Institute for High Frequency Physics and Radar Techniques. Similarly, the ESA collaborates with the European Incoherent Scatter Scientific Association (EISCAT), whose radars allow statistical observations of LEO debris down to some centimetres in size [11]. Once detected and listed the objects, several correlation processes are used for anticipating possible encounters

[1] At present, the scientific community estimates that the number of debris in the space is around 135 million [15] [February,2020]

within the space population. Among the European centres, this task is realised by the Space Surveillance and Tracking Segment (SST) [13], which catalogues debris objects, and determines and predicts their orbits. Similarly, the *18th Space Control Squadron* (18 SPCS) in the USA, once identified the **primary** (the satellite of interest), looks for all the possible convergences with its neighbourhood: **the secondaries**. When a risk is detected, it is daily monitored and three days before the possible collision the satellite operator is warned. In particular, the collected data are analysed and filtered and finally sent as a warning message called Collision Data Message (CDM) which provides all the information needed for the characterisation of the possible source of collision, included the severity of the collision probability. Indeed, when speaking about collision risk management, the issue is treated in probabilistic terms, beacause of the intrinsecal uncertainty of the problem. Considered the criticity of the issue several experts have shown their interest in developping method for the calculation of the collision probability. This is the case of Phillion in [34] who analised the results of applying a Monte Carlo method in the search of collision risk. The method studies the covariance matrix of the involved objects under consideration and is capable of estimating the relative position of the bodies with their respective uncertainties. Another important contribute was given by Chan [8], which focused on the developement of models for estimating the collision porbability for long-term encounters. Other experts investigate not only the collision risk but also the consequences of a a collision in terms of fragmentation and generation of new clouds [19]. Moreover the scientific community in the last year has been showing interest for designing missions for deorbiting debris population around the Earth. This is the case of [17] which presents passive de-orbiting missions using sails.

One last important aspect which is often analysed in this context is the proposition of methods for designing collision avoidance manoeuvres. This is the case of [17] which studies two ways for optimising an avoidance manoeuvre plan. In particular the paper proposes two different solutions: the maximisation of the relative distance of the objects at the date where the collision could occur and the minimisation of the collision probability. At the base of these strategies there is the detection of collision sources. This requires that a significant volume of data are processed, in addition to the necessary parallel elaborations (trajectory propagation, covariance propagation, listing). Consequently the collision risk management is costly in terms of computational load. For this reason, at present, these operations are handled on ground by means of powerful calculators. If on one hand this approach guarantees an accurate coverage, on the other one it strengthens the dependency link between the satellite and the on-ground station, counteracting the autonomy of the satellite.

This is what led CNES to the design of CROCO (Collision Risk On-board COmputation), an on-board software for computing the risk of collisions between the satellite and a selected spectrum of its neighbourhood. The aim is to realise a more compact system compatible with an autonomous orbit controller. Starting from a filtered list of CDM, CROCO selects a list of secondaries which enter a defined sphere of influence centred on

the primary and it computes the probability of collision. The main drawback of the system is that in order to being on-boardable it not only handles with a reduced spectrum of analysis but it also exploits calculation methods which are less performant with reference to the standard on ground one which exploits high accuracy probabilistic computations.

1.1.3 Thesis contribution: ASTERIA

This thesis work has been conceived for proposing a solution to the limitations of the two subsystems developed by CNES presented in the last paragraphs. In particular the need of coupling the autonomous controller and CROCO led to the development of **ASTERIA** (Autonomous Station-keeping Technology with Embedded collision RIsk Avoidance system): an embedded system able to perform station keeping and collision risk management at once. The system guarantees the in-track and cross-track control by means of the AOC algorithm properly adapted for the integrating the specifications of CROCO. In particular, it is conceived for building a manoeuvre horizon long enough to allow the identification of collision risk and for implementing avoidance strategies when needed.

ASTERIA is planned to be tested within the OPS-SAT mission [12], a 3-Units CubeSat proposed by the ESA for the purpose of testing innovative operational concepts.

This thesis work takes part in the realisation of this ambitious project. In particular it contributes by covering three different branches:

- the introduction of the necessary tools for realising the conceptional link between the station keeping and the collision risk analysis. This concerns in particular the addition in CROCO of an empirical model for estimating the uncertainty linked to the manoeuvres proposed by the AOC. The integration of such a model represents an important improvement in the CROCO's calculation. In consequence it represents a crucial point in the conception of ASTERIA.

- the reorganisation of the controller algorithm architecture for welcoming the risk management process. It results in an integral code which merges the 2 subsystems. The resulting system represents the accomplish of the integral version of the AOC able to guarantee a complete autonomous control. The interest in this solution is what led to take part to the OPS-SAT mission for ultimating the necessary tests and ending with an operating system. In these terms it represents an important milestone in the search of autonomy of the satellite.

- the conception of a collision avoidance manoeuvres strategy that allows the satellite to first avoid the collision and then to restore the mission once the risk is passed. Considering the growth in space population, the integration of this system is crucial and it represents a very important improvement in the AOC.

The thesis is structured as it follows:

1. **Chapter 1**: presents the scientific background of the project.
2. **Chapter 2**: describes the AOC overall strategy and the original algorithm.
3. **Chapter 3**: presents CROCO original functionalities.
4. **Chapter 4**: treats the upgrades introduced for the integration of CROCO in ASTERIA . It presents the model for the estimation of the uncertainties related to the station keeping. It also describes the integration complexities and the adopted solutions.
5. **Chapter 5** : presents the OPS-SAT mission and the ASTERIA on-board application.
6. **Chapter 6**: describes the conception of the collision avoidance manoeuvres strategy.
7. **Chapter 7**: provides a conclusive analysis of the project and presents the perspectives for further developments.

1.2 Working environment

The AOC has been developed at the Centre National d'Etudes Spatiales (CNES). CNES is the French space agency for space programs. It is a public, industrial and commercial, scientific and technical institution and it is financially independent. It is responsible for advising the government, implementing the French space policy and designing new space systems. CNES has two main missions: to provide an overall vision of space solutions through its systems skills and to innovate. In addition to this, it is attentive:

- to fulfil users' requirements
- to remain at the crossroads of scientific and technological laboratories.
- to stimulate scientific, technological, and industrial research and innovation for institutional and commercial requirements.

It is allocated in four different centres, each dedicated to complementary objectives. The headquarter is in Paris Les Halles, where all the administrative operations are managed. Administrators at headquarters, together with the overseeing ministries, establish and promote CNES policy. They also define the strategic guidelines for the agency technical centres and its relations with outside partners.
The centre in Toulouse (CST) is more focused on satellites control and orbital vehicles design and development.
The opening of the CST in 1968 was the result of the decentralization of French high-tech industries from the Paris area to the provinces. The CST replaced the former space centre at Bretigny-sur-Orge. At this key site for space research, the centre develops complete space systems with its partners in industry and the scientific community, right up to their

entry into operational service. The CST is unique in terms of its size and the diversity of its activities. It also takes part in scientific and instrumentation projects, and leads research and application programs such as Argos, Helios and Insight. It also leads the orbital system projects (satellites and on-board payloads, ground segments) and satellite station acquisition and keeping operations. It manages the technical policy and preparation of the future as well. This centre develops and executes scientific balloon-borne experiments and ensures the use of data as well as development of innovative applications.
Then, there is a centre is in Kourou, where the launch base is placed: the Guaiana Space Centre (CSG). It is dedicated to Europe's launcher program. It coordinates all resources needed for launch infrastructures, launcher and payload preparation, control of launch operations and the equipment required for launch. As well, it participates in the construction of new launch units (e.g. Ariane 6).
Finally, the Launcher Directorate (DLA) is placed in Paris Daumesnil, where the study and the development of Ariane, Soyuz and Vega launch systems are carried out. It leads all developments of new European launch systems under contract to the European Space Agency (ESA). The DLA maintains constant supervision of the launcher from production to marketing and launch, through ArianeSpace. It develops technological demonstrators to prepare for future launchers. It also leads the research on new concepts for launchers and advanced propulsion systems. This internship work has taken place in the Toulouse Space centre. In particular, it has been conducted into a division of Orbital Systems and Flight Dynamics Department, that is the Space Mechanics Service. The Orbital Systems and Flight Dynamics Department (DSO/DV) develops and carries out the studies on the space mechanics aspects, such as orbit restitution and resources localization and on the Attitude and Orbit Control System (AOCS). All the phases R&T, phases 0 and A, development phases and operation monitoring are carried out in this department. In the department one finds several divisions. One of them is the Space Mechanics Systems (MS) division. Its goals are to coordinate the support for space mechanics aspects in a project, to optimize satellite positioning and maintenance strategies for isolated or information satellites, collision avoidance, in-orbit services, interplanetary transfers and Earth re-entry.

CHAPTER 2

SCIENTIFIC BACKGROUND

In this chapter the scientific background of the project is presented. It focuses on the concepts that represent the basics of the mathematical formulation of this specific. This includes:

- A concise description of the adopted coordinate system and time scale
- The orbital characterisation with the introduction of the perturbing forces taken into account in the formulation of the problem
- The correlation between a given thrust and the evolution of the orbital parameters

The author invites the reader who wants to deeper explore the orbital mechanical fundamentals to refer to [1].

2.1 Satellite coordinate system and time scale

The reference frame which is exploited in the AOC formulation is a rotating reference frame centred in the satellite called the **TNW** coordinate system represented in figure Fig:(2.1), where:

- $\vec{T}$ identifies the tangential axis: in the direction of the satellite velocity vector.
- $\vec{W}$ is the out of plane axis: it is normal to the orbital plane.
- $\vec{N}$ lies on the orbital plane and it completes the frame according to the right-hand rule. In case of circular orbits, it lies on the same direction of the radial vector which links the Earth's centre and the satellite, but it points towards the inner part of the orbit.

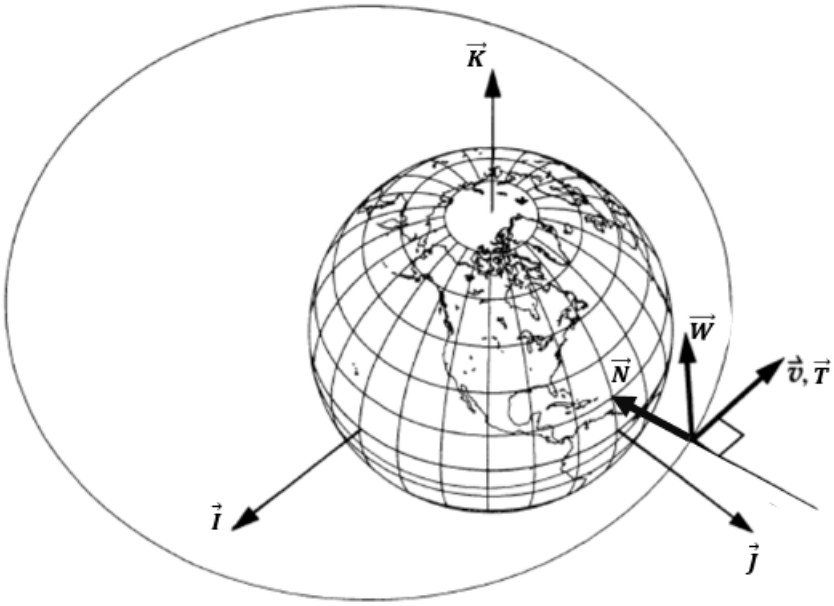

Figure 2.1: Satellite Coordinate System [7].

This coordinate system is the most adequate for the AOC because, as deeper analysed in the section Ch:(2.4), it allows to optimally express the dependency between a given thrust of the station keeping and the orbit evolution.

Concerning the temporal expression, the AOC exploits the International Atomic Time (TAI) [14]. This time scale is widely used for modelling the motions of artificial and natural celestial bodies and space applications because of its accuracy. It is based on the average time maintained from over 300 atomic clocks located in about 70 national laboratories in various parts of the world, again without introducing any astronomical correction. International Atomic Time (TAI) is an international time scale that is computed by taking the weighted average of more than 300 atomic clocks. It differs from the most known Coordinated Universal Time (UTC), which is the standard time used for all general timekeeping applications, by a simple leap second. This last is in fact based on TAI, but it is adjusted for taking into account the rotation of Earth. TAI is currently ahead of UTC by 37 seconds.

2.2 Orbital characterisation

The AOC is conceived for being adopted on different kinds of Earth centred missions (e.g. oceanography mission, observation, telecommunications). It has then been modelled for being operative on orbits which in general are:

- at low altitude: $< 2000\ km$.

- quasi circular: the eccentricity value is in the order of 10^{-3}
- Sun-synchronous. Indeed, when speaking about LEO mission, adequate and not fluctuating light conditions are usually required (e.g. for remote sensing missions). For obtaining a constant solar exposition the local hour of the passage of the satellite over a certain region is fixed. For LEO orbits the Sun synchronous orbits are almost polar.

This context led to adopt a non-Keplerian formulation for the satellite motion around the Earth [1]. The disturbing effects due to sources of acceleration different from the gravitational force are indeed significant. In consequence they can not be neglected. To take into account the presence of the perturbations effects, what is usually done, as shown in the equation Eq:(2.1) is the addition of corrective terms:

$$\ddot{\vec{r}} = -\frac{\mu}{r^3}\vec{r} + \vec{a_p} \tag{2.1}$$

According to the equation Eq:(2.1), the satellite acceleration can be seen as the composition of two terms: the first one corresponds to the Keplerian formulation and the second one is a corrective term due to perturbations. Before presenting the main sources of perturbation which characterise the orbits of interest, it is worth to remark that in a non-Keplerian orbit the concept of orbital parameters commonly used in space applications. such as parameters which do not change in time is not valid anymore. The scientific community uses to address to them as osculating parameters. For describing their evolution under the effect of perturbating terms the equations of Gauss are adopted. Differently from the Lagrange formulation (see Annex), the model proposed by Gauss consider in its formulation the presence of non-conservative forces. In consequence they are more suitable for this application. The derivation of the equations is given in [1].

2.3 Considered perturbations

The main contributes to the perturbing acceleration are given by:

- the Earth gravitational potential: the geopotential.
- the Solar radiation pressure effect, due to the photons radiated from the Sun
- the acceleration due to the atmospheric drag. When the orbit is less than 1500 km, the air molecules encounter the satellite, determining a variation of their momentum. This change creates a force acting on the surface of the satellites itself. The impact of this force depends on the local atmosphere density and on the satellite cross-section area.
- the effect of terrestrial tides: they are considered as time-varying components of the geopotential

Actually, even if it is correct to say that the AOC takes into account the listed perturbations, the way the system treats them need some ulterior clarifications:

- The geopotential, mainly due to J_2, represents a significant contribute to the perturbing acceleration. However, this contribute is already considered in the construction of the reference orbit which is not Keplerian. Then the AOC does not have to directly treat this contribute. Conversely, it will consider the terrestrial tides which, are expressed as fluctuations of the Earth potential.
- Moreover, as it will explained in the chapter Ch:(3), the autonomous controller measures the deviation between the reference orbit and the real one. This deviation is indeed caused not only by the mentioned perturbations but by any disturbing forces. So, in this sense, when evaluating the parameters variation, the AOC considers a wider spectrum of perturbations.
- Nevertheless, the AOC does use the mentioned perturbations when propagating the satellite trajectory for the creation of a future manoeuvre plan.

2.4 Orbital evolution due to a given thrust

This chapter is concluded with a brief analysis of the effects on the orbital parameters induced by an imposed thrust $\vec{F} = [F_T, F_N, F_W]$.
Starting from the characterization of the orbit done in the previous paragraph it can then be assumed that :

- $e \to 0$
- $a = r$
- $V = a \cdot n = constant$

where e is the eccentricity of the orbit, a is the Semi-Major Axis (SMA), r the radius of the orbit, V the linear speed, n the orbital angular speed.

With these assumptions, as demonstrated in [1], the Gauss equations for the description of the orbital elements assume the following formulation:

$$\frac{de_X}{dt} = \frac{\sin\alpha}{V} F_N + \frac{2\cos\alpha}{V} F_T \tag{2.2}$$

$$\frac{de_Y}{dt} = \frac{\cos\alpha}{V} F_N + \frac{2\sin\alpha}{V} F_T \tag{2.3}$$

$$\frac{da}{dt} = \frac{2\alpha}{V} F_T \tag{2.4}$$

$$\frac{di}{dt} = \frac{\cos\alpha}{V} F_W \tag{2.5}$$

$$\frac{d\Omega}{dt} = \frac{\sin\alpha}{V sini} F_W \tag{2.6}$$

$$\frac{d\alpha}{dt} = -\frac{\cos i \sin\alpha}{V sini} F_W \tag{2.7}$$

where α is the Argument Of Latitude (AOL) which is function of the true anomaly ν and of the argument of the perigee ω:

$$\alpha = \nu + \omega \tag{2.8}$$

In the equations Eqs:(2.2, 2.3) we exploited the fact that:

$$\frac{de_X}{dt} = cos\omega \frac{de}{dt} - esin\omega \frac{d\omega}{dt} \tag{2.9}$$

$$\frac{de_Y}{dt} = sin\omega \frac{de}{dt} + esin\omega \frac{d\omega}{dt} \tag{2.10}$$

$$\frac{d\omega}{dt} = \frac{d\alpha}{dt} - \frac{d\nu}{dt} \tag{2.11}$$

Moreover, considering impulsive manoeuvres, the system can be reformulated as [7]:

$$\Delta e_X = \frac{\sin\alpha}{V}\Delta V_N + \frac{2\cos\alpha}{V}\Delta V_T \tag{2.12}$$

$$\Delta e_Y = \frac{\cos\alpha}{V}\Delta V_N + \frac{2\sin\alpha}{V}\Delta V_T \tag{2.13}$$

$$\Delta a = \frac{2a}{V}\Delta V_T \tag{2.14}$$

$$\Delta i = \frac{\cos\alpha}{V}\Delta V_W \tag{2.15}$$

$$\Delta\Omega = \frac{\sin\alpha}{V\sin i}\Delta V_W \tag{2.16}$$

$$\Delta\alpha = -\frac{\cos i \sin\alpha}{V\sin i}\Delta V_W \tag{2.17}$$

where $\Delta V_T, \Delta V_N, \Delta V_W$ indicate respectively the radial, tangential and normal components of the vector $\Delta\vec{V}$.

These equations show how a given ΔV impact the orbital elements. In particular, from the Eq:(2.14) , it is evident then an impulse given in the tangential direction directly impacts the semi major axis. Similarly, a ΔV_W could be exploited for correcting Ω, i (eq: 2.15, 2.16). The last equation, even if it expresses a direct relation between the out-of-plane ΔV component and the variation of α does not represent a real tool in the AOC strategy. Indeed, in case of very polar orbits ($i \to 90$) the effect of ΔV_W is negligible. Moreover, the out-of-plane velocity variations are usually expensive in terms of fuel consumption, so it can be a good practice to look for alternatives when it is possible.

Chapter 3

Autonomous Orbital Control: Fundamentals and Algorithm

This chapter focuses on the description of the autonomous orbit controller developed by CNES as it was at the beginning of this project. Firstly, it presents the fundamentals of the station-keeping strategy. In a second time it describes the original algorithm.

3.1 Overall strategy

The approach adopted for the AOC system is for some aspects similar to the one which is usually chosen for a standard on-ground based orbital control. In particular both the solutions exploit the *virtual box* approach. At each instant, an abstract box is built around the theorical position of the satellite on the guidance orbit. The region of space within this box defines the spectrum of admitted deviations of the satellite position with reference to the theorical one. As long as the satellite guarantees to stay inside the box, no station keeping manoeuvres are needed. Conversely, as soon as its boundaries are overcome, the deviations from the theorical state are not acceptable anymore. For obvious reasons, the strategy is preventive rather than retroactive. It means that the controller does not wait for the threshold to be broken before reacting but it performs a station keeping manoeuvre plan which avoids as much as possible to exit the box, by forecasting in advance the satellite trajectory. In particular the AOC's box is defined by two deviation thresholds [Fig:(3.1)]:

- The first one ,ΔT_{MAX}, is in the tangential direction. Its control represents the whole in plane position management.
- The second one is in the out-of-plane direction ΔW_{MAX} and it defines the limitation to the cross-track deviations.

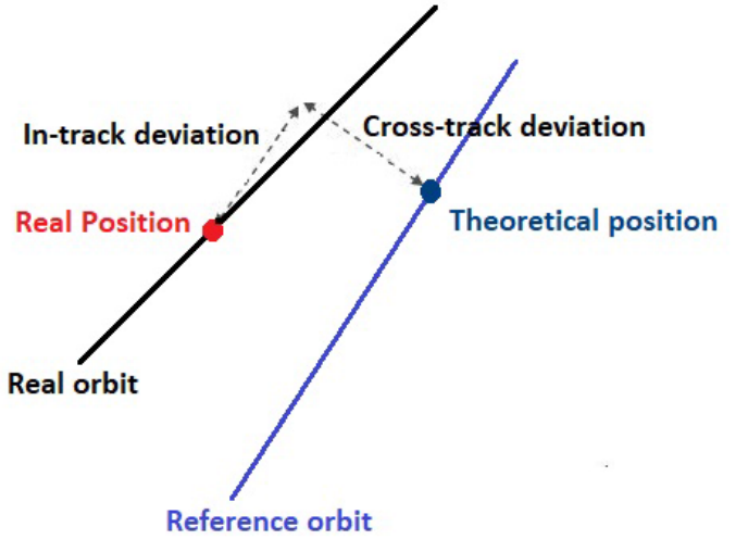

Figure 3.1: In-Track and Cross-Track Deviations [7].

Even if both strategies (on-ground and on-board) utilise this method, the second one has to handle a drastically reduced box. Consequently, less flexibility is given to the satellite's deviations. The reason of such an approach is related to communication issues between the satellite and the ground. If an autonomous controller solution is adopted, the operational centre has potentially [1]no information on the real satellite's trajectory. It knows only the theorical one. In consequence the real orbit needs to be as close as possible to the reference one for avoiding losing the communication link with the ground and for guaranteeing the fulfilment of the mission.
The figure Fig:(3.2) shows one of most evident impacts of this phenomenon: stricter are the constraints more frequent is the need of AOC intervention for guaranteeing their fulfilment. One additional peculiarity of the AOC' s methodology is that it does not directly act on the deviations ΔT and ΔW, but it exploits the thrust impact on the orbital elements shown in the paragraph Ch:(2.4). In other terms, the key idea is to translate the limitations imposed to the deviations of ΔT or ΔW in constraints on the variation of the orbital elements. Their natural evolution due to the perturbing forces is monitored and calibrated. As soon as they are forecast to produce an overcome of [ΔT_{MAX} , ΔW_{MAX}], their dynamic is analysed. If what emerges is that the situation is no going towards a stabilisation but conversely tend to amplify the critic situation, the AOC reacts by computing the necessary $\Delta\vec{V}$. The equation Eq:(3.1) represents the relation between the ΔT and the orbital elements deviation approximated at first order [7]. In particular the variation of the Right Ascension of the Ascending Node (RAAN) and of the Argument Of

[1]this is true only in theory. In practice, for reasons of robustness, the on-ground station still keeps a reduced link with the real trajectory

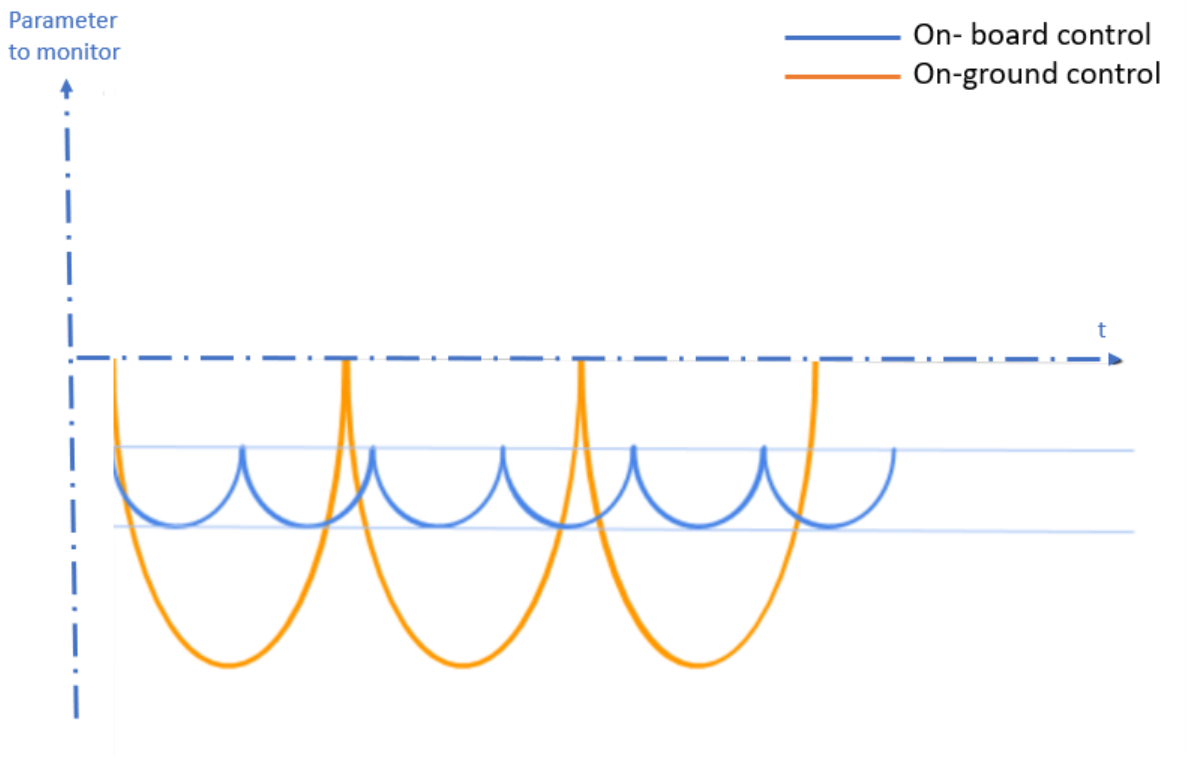

Figure 3.2: On-Ground VS On-Board Control Frequency

Latitude (AOL) are the two parameters which most influence the tangential deviation.

$$\frac{\Delta T}{a} = 2(\Delta e_x sin\alpha - \Delta e_y cos\alpha) + \Delta\Omega + \Delta\alpha \tag{3.1}$$

Concerning the out-of-plane control, the adopted gouverning equation is the following:

$$\Delta W = a(\Delta i \sin\alpha - \Delta\omega \cos\alpha \sin i) \tag{3.2}$$

As it can be seen in book by Chao [9], the ΔW can be changed by acting on Δi and $\Delta\Omega$. The approach adopted is to produce a variation of the Δi. This variation, as it will deeper explicated in the next paragraph, determines a variation of the evolution of the $\Delta\Omega$ which is then the parameter to monitor. It is also possible to act directly on the $\Delta\Omega$, but in general this solution is avoided because more expensive. Concerning the effects of the in-plane deviations on the ΔW, at the first order of approximation, they can be neglected [2].

Starting from these considerations, the AOC's strategy goes straightforward:

- it assures the cross-track station-keeping by monitoring the $\Delta\Omega$.
- once fixed the $\Delta\Omega$, it corrects the in-track deviation by calibrating the $\Delta\alpha$.

The autonomous orbital control system, according to the need, can perform three different manoeuvres:

[2] it is not the case in the opposite situation: an out-of-plane variation does involve a non-negligible evolution in the in-plane elements

LEO Missions				
Maneuver Type	Direction	Affected Parameters	Cost	Frequency
ΔV_T	$\vec{T}$	$\Delta a, \Delta\alpha, \Delta e_X, \Delta e_Y$	Low/Medium	High
ΔV_W	$\vec{W}$	$\Delta i, \Delta\Omega, \Delta a$	High	Low
ΔV_{Mixed}	$\vec{T}/\ \vec{W}$	All	Compromise	Low

Table 3.1: Manoeuvre Types Summary

- **tangential manoeuvre**. It is used for the in-plane correction, acting in particular on the AOL and the Semi-Major Axis (SMA). But it also generates an induced effect on the eccentricity. For very low altitude missions (450-700 km) the need of correction in Δa is frequent (~2/3 times par day) due to the high atmospheric drag influence. The frequency can be even higher in case of strong solar activity.
- **out-of-plane manoeuvre**. The out-of-plane manoeuvres are used for the correction in Δi, by a proper monitoring of the right ascension of the ascending node (RAAN). Nevertheless, they entail a variation of other elements too (e.g. the semi major axis). They are notoriously expensive manoeuvres. Fortunately, thanks to the strategy adopted by the AOC for the missions of interest [Ch:(3.2)], the need of a Δi manoeuvre is much less frequent in comparison to a tangential one.
- **combined manoeuvre**. It is used in case of simultaneous necessity of both a ΔV_W and a ΔV_T. In addition to reduce the total fuel consumption, it has the advantage of realising at once the two needs. This is particular useful in case of adoption of an electric propulsion system. In this case, as detailed in the section Ch:(3.5) the total time needed for performing the manoeuvres can be significant.

In the next three paragraphs the different manoeuvres' strategies are presented in details.

3.2 Out-of-plane manoeuvres

The analysis proceeds by increasing complexity of the manoeuvre. The first one to be presented is the Out-Of-Plane (OOP) one. The parameters to monitor in this case are the right ascension of the ascending node and the inclination of the orbit. The figure Fig:(3.3) shows their natural evolution under the effect of the perturbations [3].

The secular inclination drift can be considered as linear in time, with the addition of a short periodic term due to lunar-solar attraction. It can then be expressed as it follows:

$$\Delta i = \Delta i_0 + \frac{di}{dt}(t - t_0) \tag{3.3}$$

[3] It is also possible to have the inverse situation: the inclination which naturally decreases and a concave parabolic evolution of $\Delta\Omega$

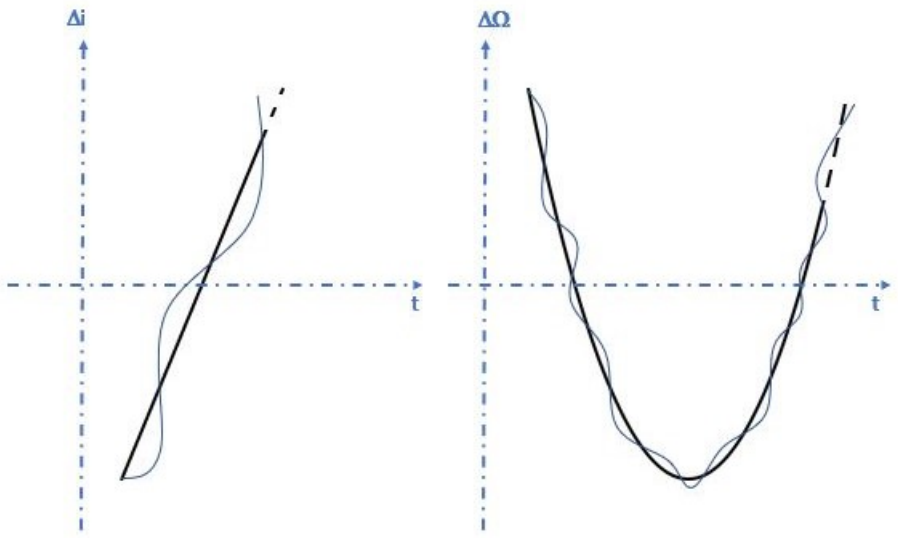

Figure 3.3: Inclination and RAAN Natural Trends

where $\frac{di}{dt}$ is evaluated considering other perturbations effects. For further information the reader can refer to the dedicated section in the annexes (Ax:I).

While the Δi is linear, the nodal drift is quadratic. Indeed according to [1] the expression of $\Delta\dot{\Omega}$ under the effect of J_2 fluctuations can be expressed by Eq:(3.4):

$$\Delta\dot{\Omega} = \frac{3}{2}\left(\frac{R_e}{a(1-e^2)}\right)^2 J_2 \sin i \, \Delta i + O(\Delta i)^2 = -\dot{\Omega} \tan i \, \Delta i + O(\Delta i)^2 \tag{3.4}$$

and considering the equation Eq:(3.3), the nodal drift can be finally expressed as:

$$\Delta\Omega = -\dot{\Omega} \tan i \, \frac{di}{dt}(t-t_0)^2 - \dot{\Omega} \, \Delta i_0 (t-t_0) \tan i \tag{3.5}$$

Showing the parabolic evolution of $\Delta\Omega$ in time[4].
The figure Fig:(3.4) represents the adopted manoeuvre strategy for the out-of-plane cross-track control.

This strategy has been conceived for both guaranteeing the $\Delta\Omega$ to always stay in an acceptable range of values and at the same time for reducing the number of performed manoeuvres and thus the fuel consumption. In this perspective, the optimal manoeuvre is performed when the $\Delta\Omega$ reaches a maximum value $\Delta\Omega_{MAX}$ which corresponds to the largest admitted cross-track deviation ΔW_{MAX}. Moreover, as represented in the left side of the figure 3.4, the manoeuvre is thought for aiming a new parabola which is tangent to the previous one in correspondence of the manoeuvre point. This implies that locally the $\Delta\Omega$ is the same; what changes is conversely its derivative. This allows to maximise the delay between the current manoeuvre and the next one. By knowing the $\Delta\dot{\Omega}_{mes}$ at the

[4]except for fluctuations due to the variation of $\frac{di}{dt}$

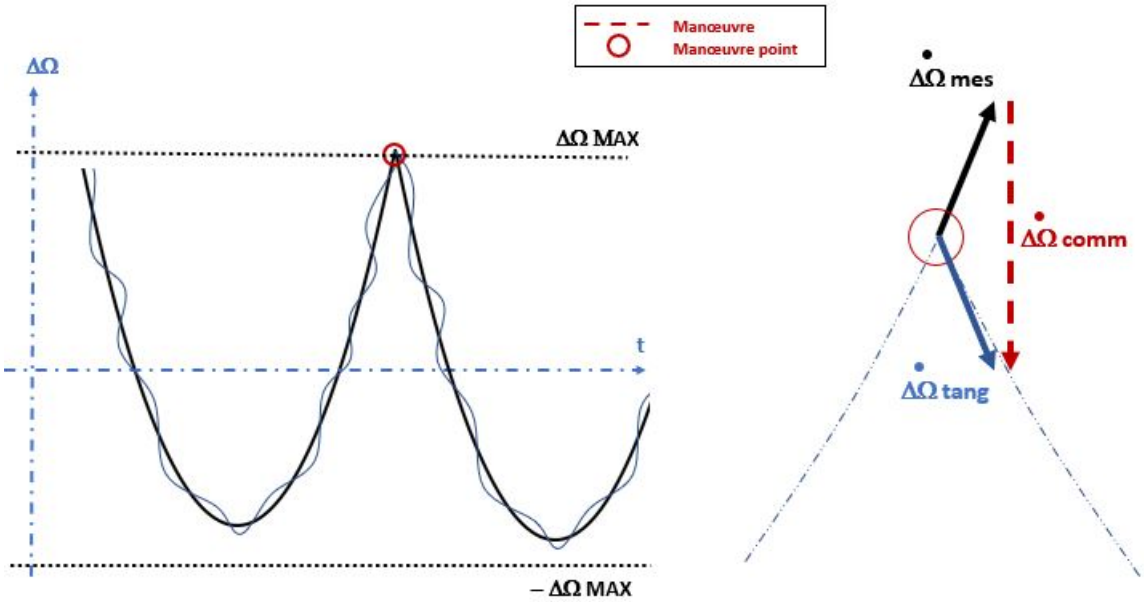

Figure 3.4: Out-of-Plane Manoeuvre Strategy

date of the manoeuvre and knowing the aimed one $\Delta\dot{\Omega}_{tang}$, the variation to impose is then:

$$\Delta\dot{\Omega}_{comm} = \Delta\dot{\Omega}_{tang} - \Delta\dot{\Omega}_{mes} \tag{3.6}$$

The given $\Delta\dot{\Omega}$ command impacts the inclination evolution as shown in the figure Fig:(3.5): the manoeuvre stops the Δi linear growth. The correspondent Δi_{comm} can be expressed as:

$$\Delta i_{comm} = \Delta\dot{\Omega}_{comm}/k_{\Omega-i} \tag{3.7}$$

where $k_{\Omega-i}$ is a scale factor between the two variables and it depends on mission specifications.

3.2.1 Manoeuvre characterisation: date and amplitude

The criteria for the choice of the manoeuvre date, $date_{\Delta\Omega_{man}}$, are here sorted by priority:

1. it must not disturb the correct progression of the mission or contrast other technical operations.
2. $date_{\Delta\Omega_{man}} < date_{\Delta\Omega_{MAX}}$; where $date_{\Delta\Omega_{MAX}}$ is the date where the satellite is forecast to overcome the out-of-plane threshold.
3. it has to correspond to an orbital position which allows to modify the $\Delta\dot{\Omega}$ without affecting the RAAN. This position is in correspondence of the two nodes, when:
   - $\alpha = 0$;

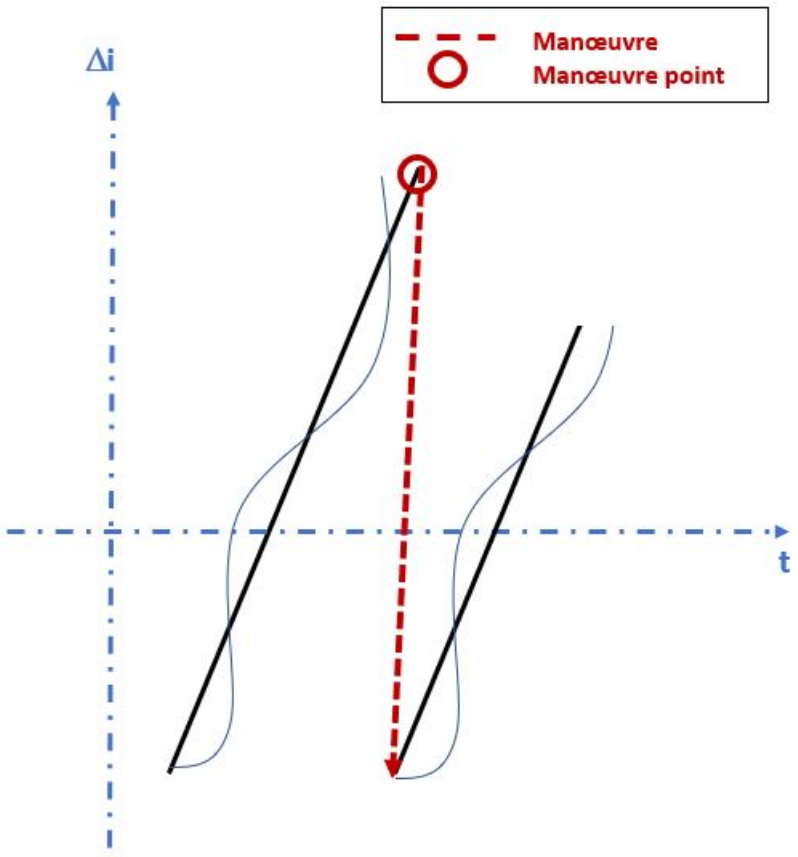

Figure 3.5: Manoeuvre Effect on the Inclination Evolution

- $\alpha = \pi$;

4. it should be as close as possible to $date_{\Delta\Omega_{MAX}}$ in order to reduce the manoeuvres frequency and indirectly the fuel consumption.

Once decided the manoeuvre point and computed the correspondent Δi_{comm}, the value of the ΔV_W to impose is expressed by:

$$\Delta V_W = 2V sin\frac{\Delta i}{2} \overset{small\Delta i}{\simeq} V\Delta i \tag{3.8}$$

3.2.2 Manoeuvring thresholds definition

Because of the first three criteria presented in the last paragraph, any point on the parabola can potentially be a manoeuvre point. Nevertheless, the strategy remains the same: aiming the parabola which is tangent to the current one in correspondence of the manoeuvre point and calculating the required command. This is always true, except for a particular case. If the manoeuvre point corresponds to the vertex of the new parabola, the equation Eq:(3.6) becomes:

$$\Delta\dot{\Omega}_{comm} = \Delta\dot{\Omega}_{tang} - \Delta\dot{\Omega}_{mes} = -\Delta\dot{\Omega}_{mes} \tag{3.9}$$

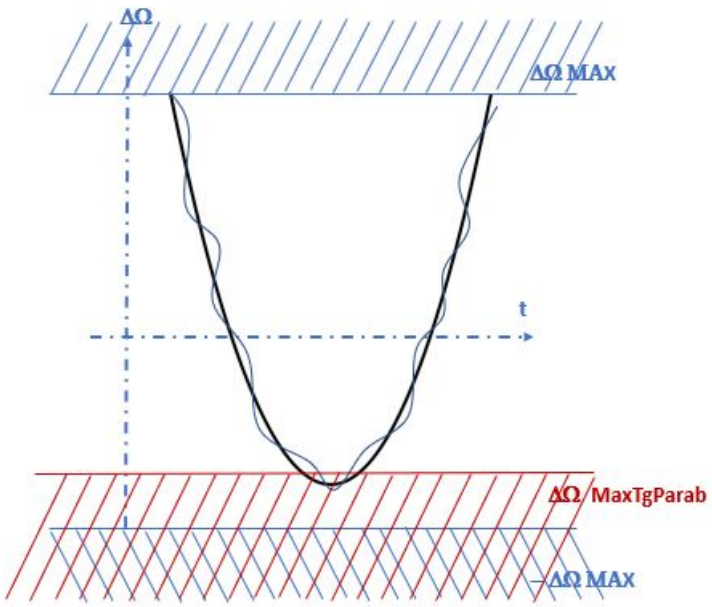

Figure 3.6: $\Delta\Omega$ Thresholds

This correction represents consequently an over-consumption because in the same direction of the natural evolution of $\Delta\Omega$. So, in order to avoid this situation, a new boundary parameter is introduced: $\Delta\Omega_{MaxTgParab}$ [Fig:(3.6)]. In summary, as shown in the figure Fig:(3.6), there are two limitations:

1. $\Delta\Omega_{Max}$; it is the deviation in Ω which corresponds to the largest accepted ΔW (ΔW_{MAX}) [5].

2. $\Delta\Omega_{MaxTgParab}$; it represents the forced vertex to the parabola; it is imposed for preventing to fall in the situation described by the equation Eq:(3.9). Its value is defined as a percentage of $\Delta\Omega_{Max}$.

3.3 In-plane manoeuvres

The strategy for the calculation of the In-Plane (IP) manoeuvres [7] is similar to the one just described, except for the fact that the ΔV_T generates an induced effect on the Δe which cannot be neglected. This issue is further analysed in the next paragraph.

The orbital elements of interest in this case are $\Delta\alpha$ and Δa. Their natural evolutions are represented in the figure Fig:(3.7).

Again, we have a linear evolution for Δa and a quadratic one for $\Delta\alpha$. Indeed, according to [1], the evolution of $\Delta\dot{\alpha}$ can be expressed by:

$$\frac{1}{\dot{\alpha}}\Delta\dot{\alpha} = \frac{3}{2a}\left[1 + \frac{7}{2}J_2\left(\frac{R_e}{a}\right)^2(4\cos i^2 - 1)\right]\Delta a - 6J_2\left(\frac{R_e}{a}\right)^2 \sin 2i\ \Delta i \tag{3.10}$$

[5] actually for robustness reasons an ulterior margin is taken.

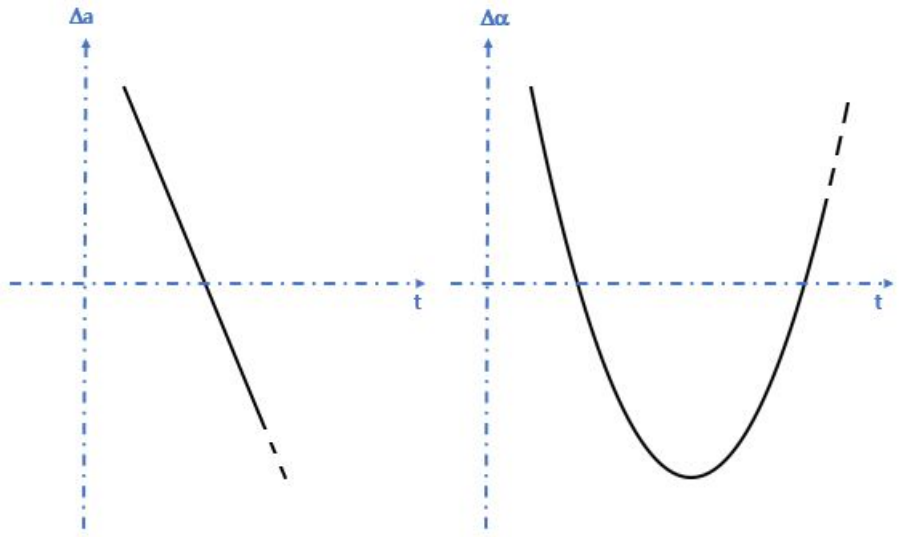

Figure 3.7: SMA and Argument of Latitude Natural Trends

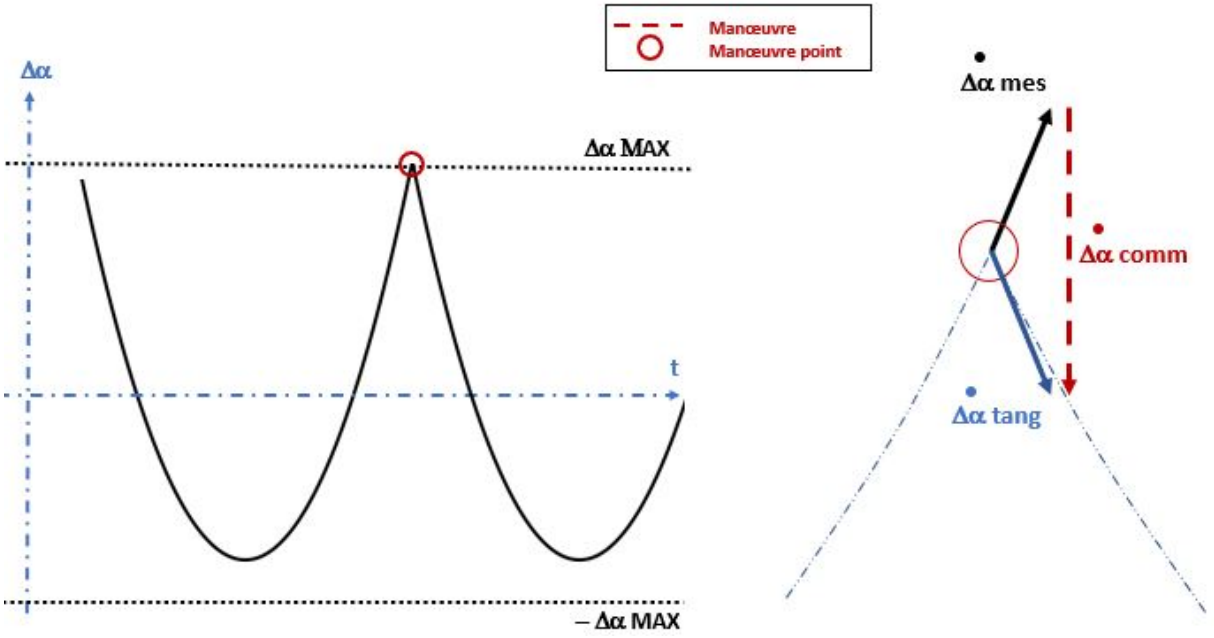

Figure 3.8: In-plane Manoeuvre Strategy

Since both the inclination and semi-major axis drifts are linear, the argument of latitude evolves parabolically in time. In the figure Fig:(3.8) the strategy adopted for the in-track control is represented. It is indeed very similar to the one used for the previous case: to perform a manoeuvre before than $\Delta\alpha$ reaches an imposed threshold $\Delta\alpha_{Max}$, targeting a new parabola which is tangent to the current one. Similarly to the cross-track control, the command in $\Delta\dot{\alpha}$ to impose is then:

$$\Delta\dot{\alpha}_{comm} = \Delta\dot{\alpha}_{tang} - \Delta\dot{\alpha}_{mes} \tag{3.11}$$

The relative semi-major axis variation is:

$$\Delta a = \frac{\Delta \alpha_{\dot{comm}}}{k_{\alpha,a}} - k_{\alpha,i}\frac{\Delta i}{k_{\alpha,a}} \tag{3.12}$$

where$k_{\alpha,a}$, $k_{\alpha,i}$ are empirically defined and they depend on mission specifications

3.3.1 ΔV_T and eccentricity deviation

Reverting the equation Eq:(2.14), the tangential ΔV can be expressed as [29] :

$$\Delta V_T = \frac{\Delta a}{2a} V \tag{3.13}$$

According to Eqs:(2.12, 2.13), this ΔV_T necessarily impacts the eccentricity of the orbit. This is what slightly complicates the management of this manoeuvre type in comparison to the out-of-plane one: the tangential manoeuvre must be computed by considering that the orbit must be kept as circular as possible. This represents a new constraint which results in the definition of an optimal argument of latitude $\alpha_{optim} = \arctan\frac{\Delta e_Y}{\Delta e_X}$. If the manoeuvre is performed in correspondence of this specific α, then the Δe is minimised. The eccentricity correction caused by an imposed tangential ΔV_T can be expressed as:

$$corr_{ecc} = \Delta e - \sqrt{\Delta e^2 + \Delta e_{man}^2 - 2\Delta e \Delta e_{man} cos(\alpha_{real} - \alpha_{optim})} \tag{3.14}$$

where:

$$\Delta e_{man} = \frac{2}{V}\Delta V_T \tag{3.15}$$

According to this expression, greater is the ΔV_T, greater is the impact on the eccentricity. In consequence when a manoeuvre in ΔT is required, the AOC

- checks that the computed ΔV_T does not comport an excessive deviation in eccentricity.
- tries to set the manoeuvre in correspondence of the optimal argument of latitude by always giving the priority to the mission.

3.3.2 Manoeuvring thresholds definition

For the tangential manoeuvres the $\Delta\alpha$ limitations [Fig:(3.9)] are represented by:

1. $\Delta\alpha_{MaxUp}$: it corresponds to the largest accepted ΔT in the positive $\vec{T}$ direction (SMA_{UP}). [6].
2. $\Delta\alpha_{MaxDown}$: it corresponds to the largest accepted ΔT in the negative $\vec{T}$ direction(SMA_{DOWN}).
3. $\Delta\alpha_{MaxTgParab}$: it represents the forced vertex to the parabola. It is adopted for preventing the critical situation: $\Delta\dot{\alpha}_{comm} = -\Delta\dot{\alpha}_{real}$ which would comport an over-consumption in fuel. Its value is defined as a percentage of $\Delta\alpha_{Max}$

[6] also in this case, as the out-of-plane one, a margin is taken

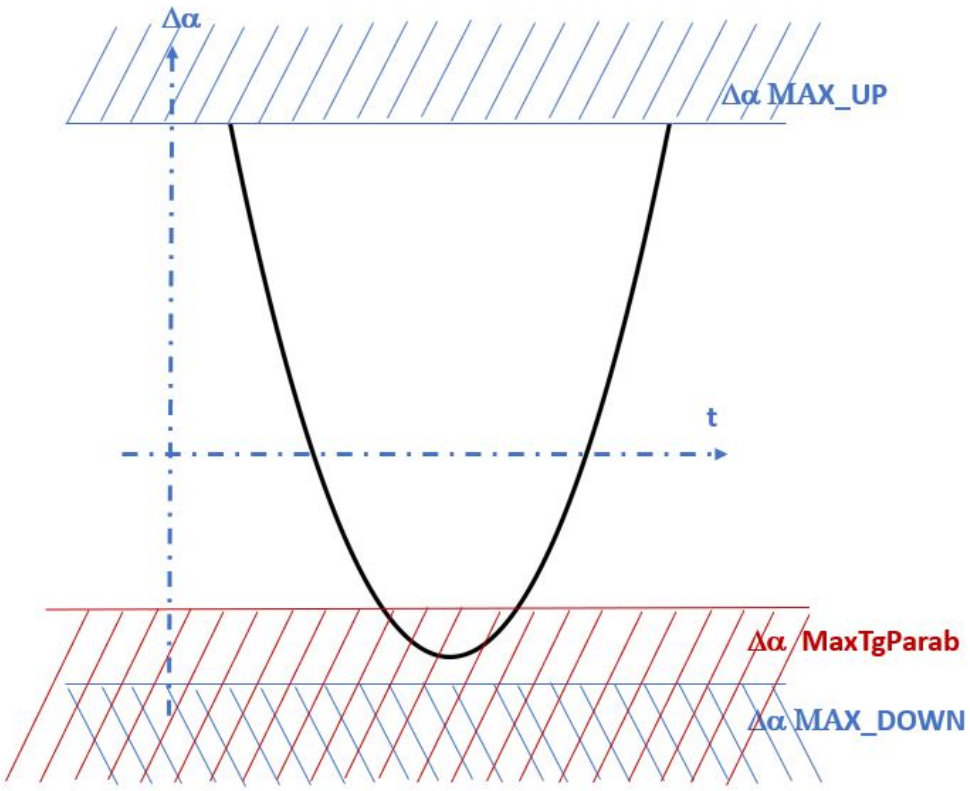

Figure 3.9: $\Delta\alpha$ Thresholds

3.4 Combined manoeuvres

In this section the last manoeuvre type is analysed: the mixed one. This manoeuvre not only allows to perform both in-track and cross-track corrections in once, but it shows to be convenient for reducing fuel consumption. The equation Eq:(3.16), remarks that a ΔV is always inferior in amplitude than the sum of the amplitudes of its two components.

$$\sqrt{\Delta V_T^2 + \Delta V_W^2} < |\Delta V_T| + |\Delta V_W| \tag{3.16}$$

It is evident that combined manoeuvres are meaningful when both an in-plane and an out-of-plane correction is needed. Actually, they are more convenient when the in-plane correction is in the positive $\vec{T}$ direction (SMA_{UP}). In fact, as shown in the figure Fig:(3.10) an out-of-plane manoeuvre induces a positive variation of the semi major axis. The reason of this phenomenon is that the given ΔV_W inevitably produces a variation in the direction of the velocity vector (and thus of the $\vec{T}$ axis) [7]. The resulting velocity in the new $\vec{T}$ direction is larger in amplitude in comparison with the initial one.

In this sense the mixed manoeuvre can be seen as an emphasis of the SMA increase induced by a ΔV_W.

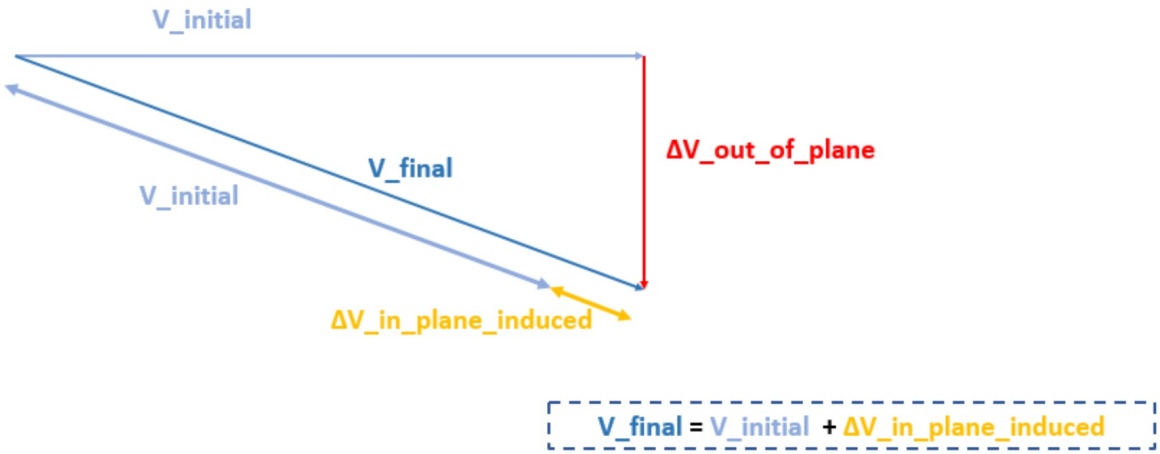

Figure 3.10: Δa induced by an OOP manoeuvre

For this reason the mixed strategy is the following: when the need of an out-of-plane manoeuvre (ΔV_W) is detected, the AOC checks if also a SMA_{UP} one is advisable. If it is the case, defined $V_{initial}$ the theorical velocity amplitude at the manoeuvre date, and $\Delta V_{T_{target}}$ the required SMA increment, the AOC:

1. computes the induced tangential variation by means of the equation Eq:(3.17):

$$\Delta V_{T_{induced}} = \sqrt{V_{initial}^2 + \Delta V_W^2} - V_{initial} \tag{3.17}$$

2. computes the needed increment in ΔV_T:

$$\Delta V_{T_{comm}} = \Delta V_{T_{target}} - \Delta V_{T_{induced}} \tag{3.18}$$

The resulting $\Delta\vec{V}$ needed to perform the manoeuvre is: $\Delta\vec{V}_{mixed} = [\Delta V_{T_{comm}}, 0, \Delta V_W]$.

3.4.1 Combined manoeuvres constraints

$\Delta\vec{V}_{mixed}$ is subjected to limitations in:

- amplitude, due to the propulsion system performances and the eccentricity constraints on its tangential component.
- direction. The angle γ between $\Delta\vec{V}_{mixed}$ and the orbital plane must stay in an admissible range. This last one depends on several elements, but the most influent one is the relative position between the satellite and the Sun. For further information the reader can refer to [7]. What is important to retain in this context is that the solar exposure is a delicate topic for space missions. According to the positioning of specific instruments or more in general the satellite design, there exists a threshold value for γ (γ_{MAX}), beyond which the subjection to the solar rays becomes problematic. This limit value, depending on the satellite exposure, varies with the orbital

position[7]. In any case, since the ΔV_W is fixed, this results in a limitation on the tangential component: $\Delta V_T \in [\Delta V_{T_{induced}}; \Delta V_{T_{max}}]$.

In conclusion, the mixed manoeuvres must meet several requirements which make their effective realisation complicated. However, for avoiding being too strict, when the two standard manoeuvres are simultaneously needed but a mixed manoeuvre is not possible, the AOC proposes other parallel solutions, which are in order of proposition [7]:

- a reduced mixed manoeuvre + a standard in-plane one.
- a standard out-of-plane manoeuvre + a in-plane one.
- a standard out-of-plane manoeuvre (if no in-plane manoeuvre is found).

3.5 On-board propulsion system

Although the orbital controller has been initially conceived for working with a chemical propulsion system, in a second time its algorithm has been upgraded for being operational also if the satellite is propelled by a low thrust electrical system. While in the first case the manoeuvres are considered to be quasi-impulsive[8], in the second one the assumption is not acceptable anymore.

The transition between the two propulsion systems has been possible by considering the electrical manoeuvre as a high-degraded impulsive one. I Looking at the illustration in the figure Fig:(3.11), it is possible to integrate all the real manoeuvre's contributions and express the relation between an impulsive ΔV_{imp} and a real one ΔV_{real} as follows:

$$\Delta V_{real} = \int_{\alpha_{start}}^{\alpha_{end}} \frac{F}{m} \cos u \; du = \frac{F}{m}(\sin \alpha_{end} - \sin \alpha_{start}) \; \frac{m \; \Delta V_{imp}}{F} \frac{1}{\alpha_{end} - \alpha_{start}} \tag{3.19}$$

$$\Delta V_{real} = \frac{\sin \alpha_{end} - \sin \alpha_{start}}{\alpha_{end} - \alpha_{start}} \; \Delta V_{imp} = \eta \Delta V_{imp} \tag{3.20}$$

where $\eta = \frac{\sin \alpha_{end} - \sin \alpha_{start}}{\alpha_{end} - \alpha_{start}} < 1$ is the efficiency of the real manoeuvre and in this application depends on the adopted electric propulsion system. In other terms for obtaining a target ΔV_{imp} , the electrical propulsion system must perform a $\Delta V_{elec} = \frac{\Delta V_{imp}}{\eta}$.

In addition to the amplitude of the manoeuvre, there is a second important parameter that has to be taken into account when treating electrical manoeuvres: the thrust time. Starting from the Tsiolkovsky equation Eq:(3.21):

$$\Delta m = m_0 (1 - e^{-\frac{\Delta V_{elec}}{g I_{SP}}}) \tag{3.21}$$

and assuming :

- constant thrust, mass flow, specific impulse
- $\Delta V_{elec} < g I_{SP}$ [9]

[7] if not SSO.
[8] quasi-impulsive: the ΔV is corrected by an efficiency term and a thrust time is considered
[9] normally for electric propulsion systems, $I_{SP} \sim 10^6 s; \Delta V_{elec} \sim 50 - 100 km/s$

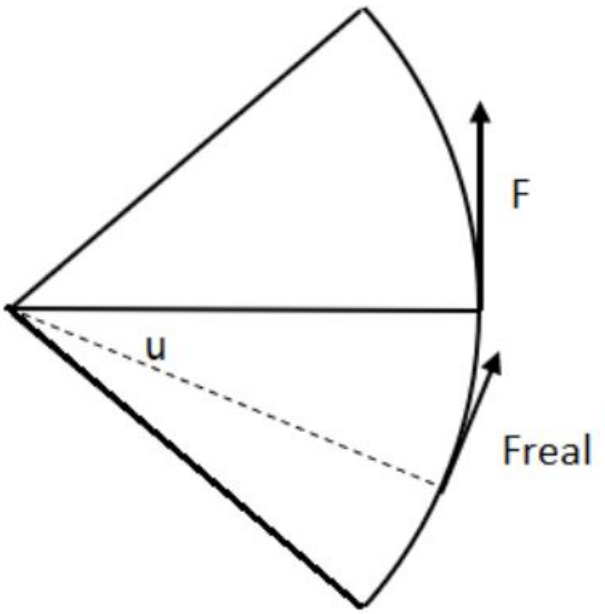

Figure 3.11: Electical Thrust Formulation [17].

the equation Eq:(3.21) becomes

$$\Delta m = m_0 \frac{\Delta V_{elec}}{g I_{SP}} \tag{3.22}$$

then the required time is:

$$\Delta t = \int_{m0}^{m_{fin}} -g\frac{I_{SP}}{F} dm = -g\frac{I_{SP}}{F}\Delta m = \frac{m_0\ \Delta V_{elec}}{F} \tag{3.23}$$

Once defined the Δt and the efficiency η, the transition between the two propulsion systems is obtained as follows:

1. When a manoeuvre is required, its ΔV_{imp} and the respective ΔV_{elec} are established.

2. A temporal horizon analysis starts: the AOC takes into account the available time segments in which it is possible to perform station keeping manoeuvres and, according to the manoeuvre type, it sorts them by using the criteria previously described in the paragraphs Ch:(3.2.2, 3.3.1).

3. By reverting the equation Eq:(3.23), the algorithm goes through the slots determining the largest ΔV that can be imposed in each one and it spreads the required ΔV_{elec} up to its complete extinction.

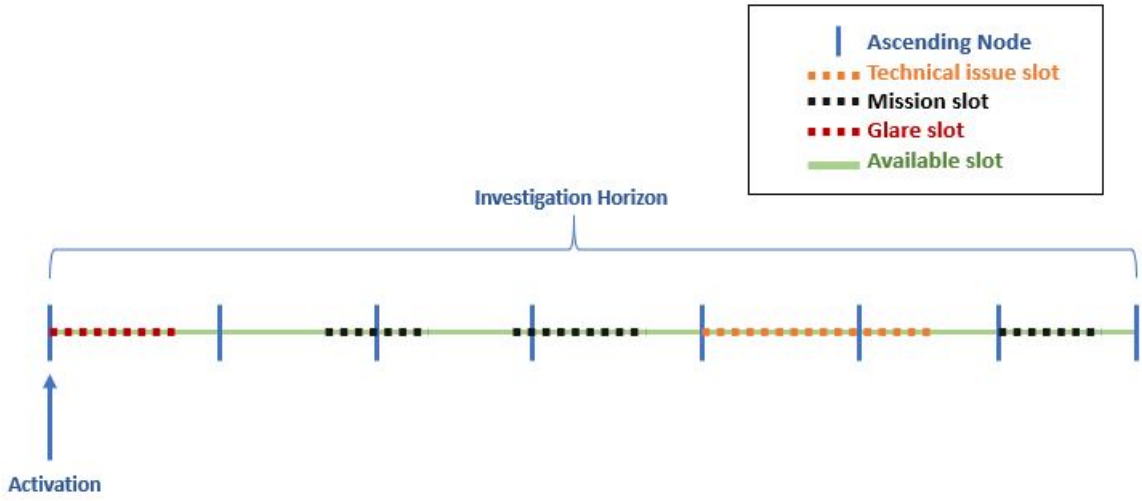

Figure 3.12: AOC Time Investigation Horizon

3.6 Temporal horizon of investigation

Before presenting the algorithm, it is worth to spend some words on the investigation temporal horizon. Indeed, the characterization of this horizon is in itself a crucial point in the conception of the AOC [17]. First of all, it must be said that within the whole temporal window which is analysed by the AOC, only some segments are really consecrated to station keeping purposes. The rest of this horizon cannot be accessed because exploited for other reasons:

- for technical operations (e.g. the recoiling of the engine, or the thrusting positioning and the thrusting time)
- because of disturbing glare conditions.
- for the realisation of the mission. This last one indeed has always the priority on the station-keeping. On one hand this approach guarantees that the orbital maintenance does not disturb the mission, on the other ot could not be the best strategy in case of the detection of a collision risk by the ground station.

For all these reasons , as shown in the figure Fig:(3.12) the number of temporal windows available for station keeping purposes is limited .

The total length of the horizon considered for creating the manoeuvre plan is about a day. This represents a compromise between two parallel needs. The longer is its duration, the more is the time given to the collision risk management system for detecting a danger and react. However, a lower temporal interval is characterised by more accurate data. Moreover, while a long analysis period is auspicable for a on-ground control, where there

is always a delay between the satellite and the station, the reactivity of an embedded solution does not require this constraint anymore.

As shown in the figure Fig:(3.13),we distinguish two main parts in the investigation temporal window: the **predictable horizon** and the **research horizon**.

Predictable horizon

This first interval, which starts at the activation date, contains the manoeuvres which have been calculated at the previous activations. [10] It is further split in [7]:

- a Frozen Horizon (FH): the manoeuvres within this segment are completely fixed, they cannot be changed anymore.
- a Semi-Frozen Horizon (SFH): the manoeuvres which are contained in this second window can be partially updated. In particular they can change in amplitude but not in direction and in date.

This repartition has been conceived as a compromise between two not compatible needs. The first one, as previously anticipated, is related to the risk of collision: the more flexible, the less predictable is the plan. The uncertainty linked to a horizon that can completely change, drastically complicates the risk calculation. This led to fix the manoeuvres which are closer in time. The second one is the need of allowing some flexibility and reactivity of the controller system. This is particularly important for managing the effects of the unpredictability of the solar activity, which makes a global frozen solution too severe.

Research Horizon

The end of the predictable segment represents the starting point of the research horizon. It is investigated and as soon as one of the thresholds is broken, the relative corrective manoeuvre si calculated.

3.7 AOC algorithm

The autonomous control system is activated at each ascending node. The reason why the ascending node has been selected is because, conversely to the poles, it is in a low visibility latitude zone from the ground stations. This normally guarantees to not interfere with mission's operations. In the following paragraphs the steps for the composition of the manoeuvre plan are described.

3.7.1 Orbital deviation and predictable horizon analysis

At the activation, the AOC obtains the information of its real orbital state and it compares it with the theorical one on the reference orbit. It then exploits its past history of the

[10] except for the very first activation which has to integrally build the manoeuvre plan

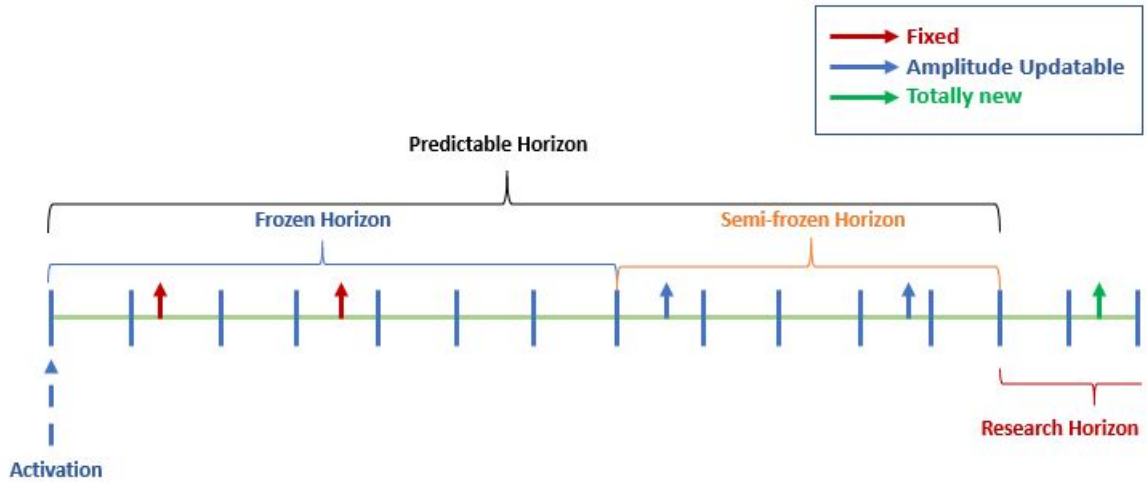

Figure 3.13: Investigation Horizon Segmentation

stored deviations for modelling the trend of Δe_x, Δe_y, $\Delta\Omega$, $\Delta\alpha$. In particular, the evolutions of Δe_x, Δe_y are considered linear; the evolutions of $\Delta\Omega$, $\Delta\alpha$ are parabolic. By means of a polynomial fitting [7], also $\dot{\Delta e}$, $\dot{\Delta\Omega}$, $\dot{\Delta a}$, $\dot{\Delta\alpha}$, $\ddot{\Delta\alpha}$ are estimated. Their values are fixed through the entire horizon and they will be updated at the next activation. At the end of this first step the AOC has all the tools for proceeding with the station-keeping plan construction.

1. Starting from the activation date, it performs an analytical propagation through the frozen horizon. In this propagation it always considers the impact of the potential manoeuvres that it encounters on this path. It is important to keep in mind that the manoeuvres inside this temporal segment rest unchanged and they will then be performed by the satellite.

2. The semi-frozen horizon offers a greater flexibility to the AOC. Indeed, while performing a second propagation, the AOC has the possibility to eventually update the manoeuvres. The ones who fall in the very first orbit after the FH are checked and eventually corrected in amplitude: $\Delta V_{MAN} \in [\Delta V_{MIN} \Delta V_{MAX}]$.

3.7.2 Research horizon analysis and next manoeuvre determination

Once left the SFH, the system has complete freedom[11] in the computation of the next station keeping manoeuvre. So it extends its propagation up to the detection of the new manoeuvre to perform, identifying both the manoeuvre type and the **critical date**: the threshold crossing date. The next steps depend on the next manoeuvre type.

[11] except for the mission and technical constraints

- *in-plane manoeuvre*: this manoeuvre can be performed by adopting two different criteria: the minimisation of the eccentricity degradation, or the optimisation of the ΔV. For determining which approach assuming, the AOC calculates the value of Δe_{man} at the critical date and it compares it with the current value $\Delta e_{activation}$. If the number of manoeuvres for achieving Δe_{man} is greater than a specific limit value n ($\Delta e_{activation} > n\Delta e_{man}$), then the adopted criterium is the eccentricity one. Otherwise the dimensioning criterium is the ΔV optimisation.
  In both cases, the available slots between the end date of the SFH and the limit one is analysed in chronological order. The AOC looks for the one which represents the best compromise between the manoeuvre date and the AOL value, which should be as close as possible to α_{optim} [Ch:(3.3.1)]. If, conversely, no slot is found before the critical date, the research continues afterwards. As soon as an acceptable slot is found, it is selected no matter the cost in eccentricity.

- *out-of-plane manoeuvre*: the available slots are analysed backward: from the critical date to end of the SFH. as soon as an appropriate slot is found then, the research is interrupted.

- *mixed manoeuvre*: the algorithm checks if in correspondence of the ΔW_{MAX} crossing date, a mixed manoeuvre is needed. If it is the case, it tries to add a ΔV_T component to the final $\Delta\vec{V}$ vector. At this point there are three criteria to optimise: to minimise the induced Δe, to fulfil the needs in $\Delta V_W, \Delta V_T$ and to delay as much as possible the manoeuvre.
  The out-of-plane component has the priority. So, the algorithm firstly looks for the slots$_W$ which allows the required ΔV_W. For each of them it computes maximum available $\Delta V^i_{T_{MAX}}$ and it compares it with the ΔV^i_T needed at that specific date.
  If $0 < \Delta V^i_T <= \Delta V^i_{T_{MAX}}$, the mixed manoeuvre is created: ΔV_{MIX}=[ΔV^i_T, 0 , ΔV^i_W] and it is added to the horizon.
  If, $\Delta V^i_T = 0$ or$\Delta V^i_T > DeltaV^i_{T_{MAX}}$, the research horizon is again examined looking for a slot$_T$ for the tangential component. Once found it, the algorithm checks if it is also possible to split it in two parts, one to fix in the current slot and the other to add to the normal component for having a mixed manoeuvre. If no slots for the tangential component is found, the algorithm passes to the following slot$_W$. It repeats this procedure up to extinguishing all the slots$_W$. At the end of the iteration it ends with a list of possible combinations among which select the optimal one.

3.7.3 Post processing of the manoeuvres research

Once concluded the horizon analysis, two scenarios are possible:

1. A next manoeuvre has been found. If it falls in the first orbit of the research orbit, at the next activation it will belong to the SFH and it will eventually be updated. Otherwise it is discarded.

2. There is no manoeuvre in the predictable horizon and no manoeuvres have been found. It means that at the next activation no more manoeuvre is included in the SFH. Even if at first sight it is a positive fact, in the long term it can be determine a decrease in station keeping performances. Indeed, if ,due to a sudden change in the environment conditions, a manoeuvre in the SFH was necessary, it would not be possible to add it because of the very same definition of this temporal segment. Even if this represent a unlikely situation, it could represent an issue. For preventing it is possible to introduced the so called **opportunity manoeuvres**. They consist in null in-plane manoeuvres which are forced to be add in the first orbit of the research orbit if the time spent from the last inclusion of a manoeuvre in the semi-frozen horizon is longer than a reference time[12]. In this way, at the next activation they will enter the SFH and they can eventually be updated if needed.

[12] the reference time depends on the solar flux activity

Chapter 4

CROCO: Collision Risk Management Fundamentals and Strategy

Speaking about collision risk calculation implies a probabilistic analysis. The same state vectors of the orbiting objects, as long as the propagation strategy are characterised by intrinsecal uncertainties. Consequently, it is no possible to know with absolute precision when a collision will occur. The accuracy of this analysis must then be intended in probabilistic terms. In the perspective of maximising the accuracy related to the collision risk management, what is usually exploited in on-ground applications is a Monte Carlo method (MCM) [21] which by using random variables, guarantes a wide coverage and very good results. Unfortunately, the drawback of this solution is that it pays its accuracy with computational times which are so long that their on-board application would be complicated and ineffective. A different numerical approach is to exploit an adaptive splitting technique for the estimation of the collision probability [24]. This approach showed to be more appropriate in case of rare events than a MCM which conversely needs a significant number of samples (10^6 points for a sought probability on the order of 10^{-4} [24]). A completely different strategy is the one proposed by Gonzalo [17] and Chan [4],based on an analitical covariance propagation rather than numerical. In particular, they simplifie the problem, by assigning a combined covariance to the debris (the sum of the individual covariances for both objects) and a combined envelope to the satellite. According to these approaches, the collision probability can be approximated to a convergent serie. The advantage of this approach lies on its analitical formulation which significantly reduces its computational cost [17].

The strategy at the root of CROCO partially sacrifiesies the accuracy level which characterises the Monte Carlo method applications, for a significant reduction in computational time. It exploits an analitical approach, which similarly to the one proposed by Patera [25] results in the reduction of the probability collision to a one dimensional

integral that permits easy numerical implementation and reduces computational effort.

4.1 Mathematical formulation of CROCO

The assumptions and the mathematical fundamentals of CROCO development are here presented.

When dealing with two-object enocunters, the scientific community usually addresses to the satellite of interest as the **primary** (p), while the objects in its proximity are the **secondaries** (s). Moreover, it usually distinguishes two types of collisions [28]:

- *short duration and high relative velocity collision*. In this case the two relative momentums can considered linear in the vicinity of the encounter. Moreover it is assumed that the velocities are deterministic.
- *slow and low relative velocity collision* . In this case the hypothesis of linearity is not valid anymore.

In this application, all the collisions are considered to be of the first type. This is approsimation has a twofold advantage. On one hand, considering that for LEO missions the satellite velocity is in the order of 8 km/s[1] it well represents the reality. On the other one it significantly simplifies the analysis. The model also assumes that:

1. The primary and the secondary are spherical and they are represented by their enclosing spheres, with respective radii R_p,R_s(Fig:(4.1)).
2. The dynamic model and probability density of the two objects are independent one from the other.
3. The probability densities for both the objects (ρ_p, ρ_s) are Gaussian [25].

With these assumptions it is possible to define a collision plane or *BPlane* [25] which contains the encounter :

- the vector $\vec{e_1}$ oriented along the relative speed of the two objects. This vector is orthogonal to the collision plane.
- the vector $\vec{e_2}$ belongs to the collision plane and is orthogonal to the plane defined by the relative mean position and relative velocity.
- the vector $\vec{e_3}$ completes the tern according to the right-hand rule.

[1] This is true for isolated satellites. It is true that the velocity amplitude on a LEO orbit is very high. But the relative velocities of the two objects in case of configuration such as train or constellations can be much lower.

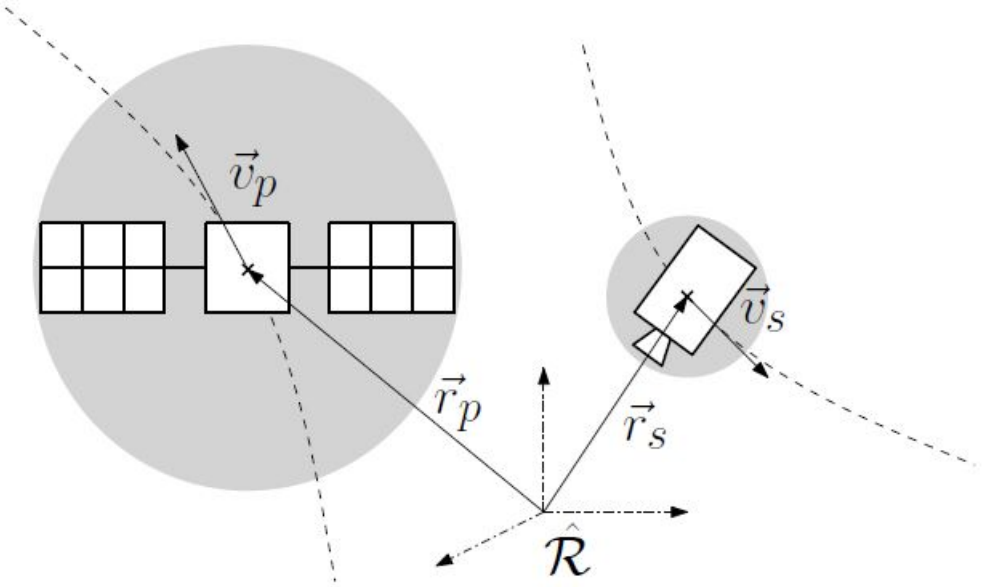

Figure 4.1: Primary and Secondary Enclosing Spheres [21].

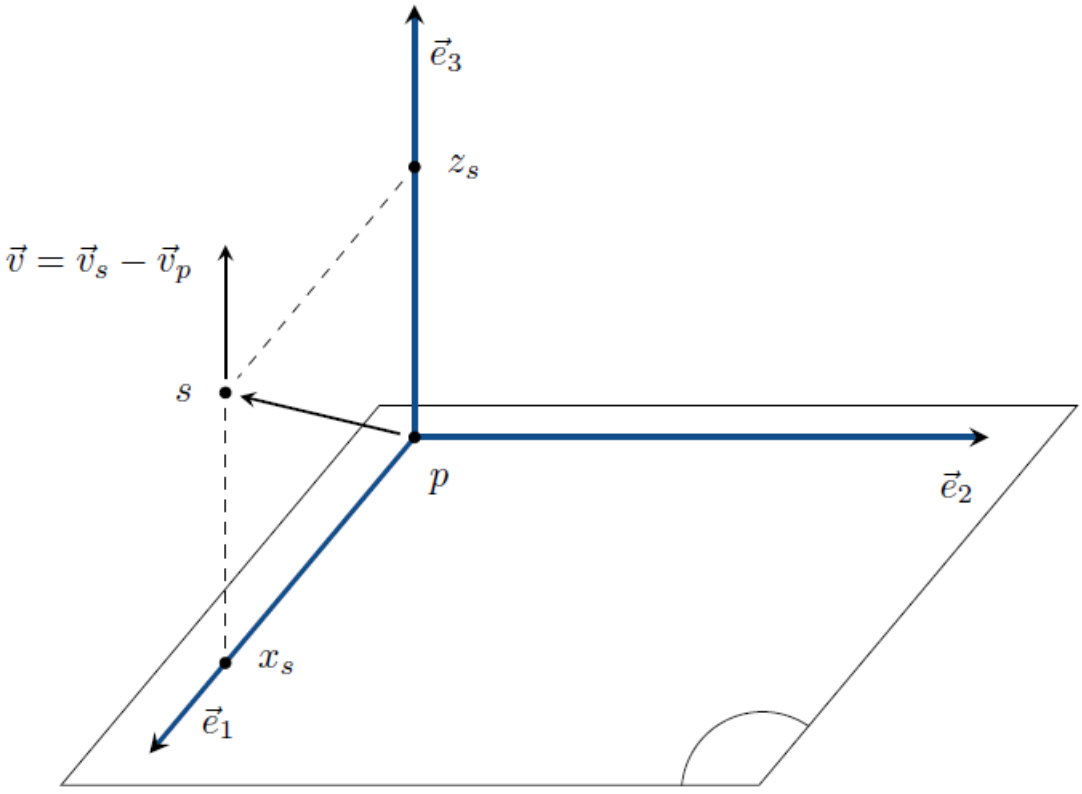

Figure 4.2: Collision Plane [27].

The tern is usually centered in the primary. The interest of the Bplane is that it simplifies the problem formulation by alllowing to translate from a three-dimensional formulation to a two-dimensional one.

Considering a temporal interval $[t_0, t_0 + T]$, the dynamic model is governed by:

$$\frac{d\vec{x_i}}{dt} = f_i(\vec{X}, t); \tag{4.1}$$

$$\vec{X} = (\vec{x_p}, \vec{x_s}); \tag{4.2}$$

$$\vec{X}(t_0) = \vec{X_0} = (\vec{x_{p0}}, \vec{x_{s0}}) \tag{4.3}$$

Where

- $i = p, s$
- $\vec{x_i} = (\vec{r_i}, \vec{v_i})$
- $\vec{X_0}$ represents the initial condition and it is in itself associated to a uncertainty, expressed by aprobability density $\rho_0 = \rho(\vec{X_0}, t_0) = \rho_p(\vec{X_0}, t_0)\rho_s(\vec{X_0}, t_0)$

The last important parameter for the analysis formulation is the *probability threshold* P_{thsd}. It represents a specification of the model and it exprimes the boundary between a no risky situation and a risky one. The problem is then espressed as follows: given a certain P_{thsd} we are interested in finding the ensemble E of the initial conditions which result in a collision probability P_{coll} which is greater or equal to the threshold value. This is mathematically espressed by:

$$P_{coll} = \int_E \rho_0(\vec{X_0}, t_0) d\vec{X_0} >= P_{thsd} \tag{4.4}$$

4.2 CROCO application: OPS-SAT and ANGELS

This paper has already presented the outline of the mission OPS-SAT in the paragraph Ch:(1.1.3), which will be exploited by CNES for the realisation of test campaigns. Among them, the CROCO application experience aims to investigate the feasability and the on-boardability of the system.

However the installation is limitated by accessibility restrictions: the Operetional Orbitoghraphy Centre (COO) of CNES has not currently access to the CDM's of OPS-SAT which is instead managed by the ESA. It means that the information on Cube-Sat neighboroohd is not available. Nevertheless, CROCO has been conceived for being functional regarderless the satellite which implements it. Thus, the solution adopted for the realisation of the experience is the following: to exploit the data of a different mission tracked by the CNES and adapt them to OPS-SAT. The selected mission is called ANGELS (Argos Neo on a Generic Economical and Light Satellite) a nano satellite promoted by CNES in collaboration with Hemeria. [26]. The reason of this choice is evident if looking

at the table Tab(4.1) [2]: the two missions have extremely similar guidance orbit and they have been launched at the very same time. The idea at the base of this approach is that

Satellite	Perigee z $[km]$	Apogee z $[km]$	Inclination $[°C]$	Period $[min]$	SMA $[km]$
OPS-SAT	516.0	536.8	97.5	95	6897
ANGELS	514.8	533.0	97.5	95	6894

Table 4.1: Compairison between OPS-SAT ans ANGELS orbits

what can potentially be a risk for ANGELS will be a risk for OPSSAT too. So ANGELS is used only for the purpose of recovering the CDM of the risky secondaries which can represent a danger for OPS-SAT too. The recovered CDM information is obviously centred in ANGELS, in particular the potential risks are dated in correspondence of their TCA with ANGELS. However with a coupling of backward and forward propagations it is possible to refer them to OPS-SAT.

4.3 CROCO strategy

In this paragraph the CROCO functionning is presented in details. There are two main phases: the on-ground segment and the on-board one.

4.3.1 Ground phase

This first phase is necessary for providing the satellite of all the information concerning the secondaires in the near space. For this purpose the COO investigates a list of CDM to transfer to the on-board system. Three main factors impose limitations on the data volume that can be sent to OPS-SAT: the storage capacity, the transmission time and the transmission frequency. Indeed the CubeSat is accessible by the ESA antenna only twice par day for a temporal window of half an hour.

1. **CDM Filtering Process** Once a risk is detected, the related CDM is emitted (potentially by several ground detectors) for the 7 days before the date of the risk. This allows a redundancy in the data as long as a daily update. Even if it represents an incremented accuracy in the management of the risk at ground, there is no interest to trasfer the whole information to the on board system, especially when the on board system has a limited capacity. It is thus mandatory to filter the data provided by the on ground detectors. This is exactly the preliminary operation in the CROCO's strategy: a geometrical filtering process which discards the data that are redundant by keeping the ones which are essential. Moreover, once selected the data of interest, they are ulterieurly simplified and synthetized for ulterieurly reducing their volume. The filtering has been conceived fot the purpose of guaranting

[2] where z is the altitude with reference to Earth surface

a certain flexibility level to the user. Thus the criteria used for sorting the CDM can be selected: for exemple they can be classified by generation date or by TCA.

2. **CDM Synthesis Process** Once selected the high interest events, the very same structure of the collision date messages is reformulated . Indeed, according to the mission specifications, some information contained in a standard CDM is potentially not exploited by the CROCO application, and then is discarded before the transfer to the satellite [27]. After several test campaign at CNES, the average saving that can be obtained thanks to synthetis is around the 62% [27]. Nevertheless, this purge process has been conceived for being reverseble, if one of the removed data wants to be recovered. The table Tab:(4.2) reports the information which is strictly necessary in a CDM messagge , and then that can no be discarded.

Section	Content
INTRODUCTION	Creation Date, Originator ID
RELATIVE METADATA	Horizon Length, Miss Distance, SV Sizing, SV Entry and Exiit Time
SEGMENT	Object ID, Covariance Method, Manouvrable, Geometrical Characterisation, Mass, State , Covariance

Table 4.2: Collision Data Message Structure (SV: Screen Volume)

4.3.2 On-board phase

Once that the ground station have transferred the filtered CDM, the on board phase starts. It inclueds the configuraton, the ANGELS-OPSSAT conversion and the probaility computation with the covariance propagation.

1. **OPS-SAT Configuration and trajectory propagations**. The table Tab:(4.3) shows the configuration data for the initialisation of CROCO.
   First of all, the CDMs , initially centred on ANGELS need to be referred to OPS-SAT. For this purpose, a retroprogation is conducted on the secondary for recovering its state in correspondance of the OPS-SAT Orbit Determination (OD) date. Then, both

Configuration Data	Description
Horizon characterisation	The starting and ending date of the temporal window
Primary CDM	The data on the primary (OPS-SAT) at the OD date
Secondary CDM	The previously filtered CDM list centred on ANGELS
Screen box configuration	Definition on the collision analysis specification

Table 4.3: CROCO configuration data

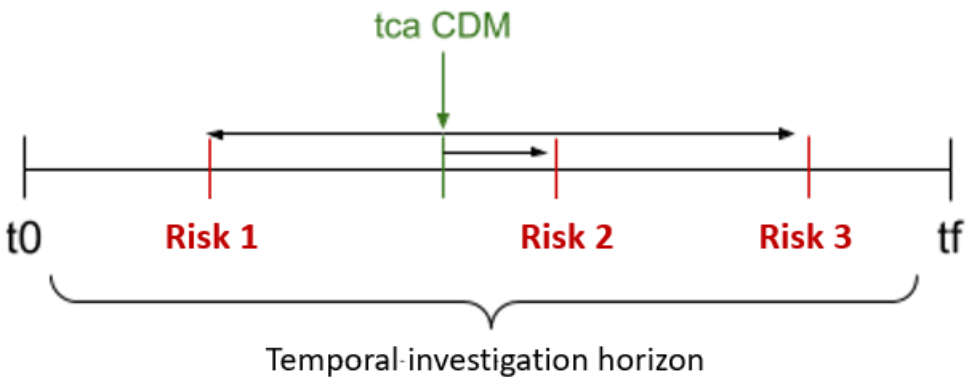

Figure 4.3: CROCO's propagation scheme

the primary and the secondary states are propagated in the future up to when a local minimum in the distance between the 2 objects is attaint, t_{min_i}. If the mimimum is before the end of the domain of interest, the propagation restarts from the current t_{min_i} and the process is iterated up to the end of the investigation horizon. So, finally, CROCO returns a list containing the local minima min_i between the two objects. Before proceeding with the probabilistic computation, the list is further filtered. Indeed, among all the minima that have been detected during the propagation only the ones that in their trajectory enters a delimeted region of space in the vicinity of OPS-SAT are kept, all the others are discarded. At the end of this process what CROCO has a list of potential risks. The next step is the computation of he probability of collision.

2. **Probability computation**. For each risk, the algorithm derives the covariance of the two objects at the risky date. This represents a complicated issue because it requires a propagation which for the secondaries starts at the TCA contained in the original ANGELS CDMs up to the relative t_{min_i} derived at the previous step. A scheme of this procedure is given in the figure Fig:(4.3).

   Where:

   - t_0 the date returned by the OPS-SAT OD;
   - $tcaCDM$ the TCA date between the secondary of interest and ANGELS;
   - t_{min1}, t_{min2},t_{min3} local distance minimum between the primary and the secondary

   At the end of the analysis CROCO returns to the ground station a list of CDMs containing the high interest risks.

Chapter 5

ASTERIA Conception

What described so far represents the base this project has been developed on.
The table Tab:(5.1) summarises the advantages and the limitations of the two embedded systems. It is time to focus on the integration of CROCO inside the autonomous control system. This chapter covers the following points:

- the upgrade of the global architecture of the autonomous orbital controller in the optic of including CROCO's algorithm and the premises for the introduction of a new functionality for the collision avoidance.
- the presentation of the missions of interest used for the simulations.
- the introduction of the last tools for a proper communication between the two subsystems. This concerns in particular the introduction of a model for estimating the uncertainty linked to the manoeuvres plan.
- the realisation of the global architecture of ASTERIA with the analysis of the effects on the algorithm. In particular, attention is given on the consequences in terms of computational load and consequential considerations.

System	Advantages	Disadvantages
AOC	autonomous control predictable horizon mission guaranteed	no reaction in case of risk detection
CROCO	embedded system reduced computational cost	no criteria for the risk gravity determination no knowledge of the orbital maintenance

Table 5.1: AOC & CROCO Recap

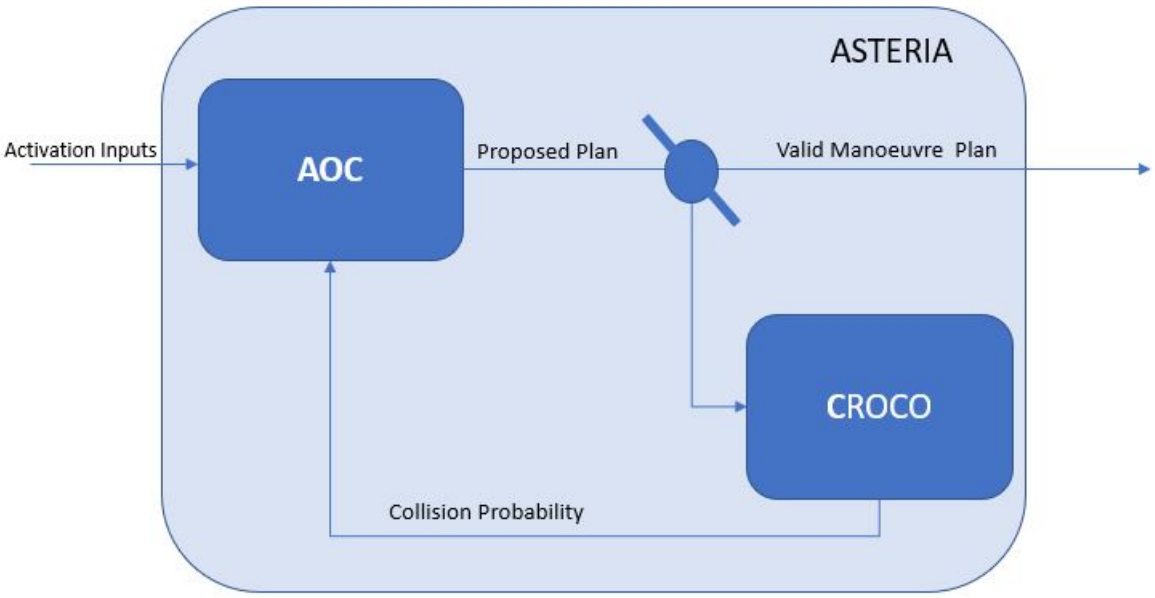

Figure 5.1: ASTERIA architecture

5.1 Towards ASTERIA: AOC upgrade

The overall algorithm strategy is presented in the schema Fig:(5.1). The upgraded AOC proposes a SK plan to CROCO, which includes the manoeuvres contribute to its analysis. It then returns an output to the controller. There are two cases:

1. **Positive Response** .The plan is no collision risky. It is then validated.
2. **Negative Response**. A risk is detected, the plan is potentially dangerous, and a solution is needed.

The upgrade of the AOC does regard this second case: if the CROCO check gives a negative result, the AOC can propose an alternative plan which implies the temporally degradation of the mission for realising an avoidance strategy.

5.1.1 Introduction of the avoidance plan architecture

What is presented in the following is the overall conception and the implementation of the architecture that in a second time will welcome the algorithm core for the realisation of the avoidance plan.
In case of the detection of a possible collision, the very same AOC's priority changes: it is not anymore to guarantee the station keeping but it is to avoid a collision, even if it implies to temporally degrade the mission accomplishment. This new configuration

does impact several aspects in the conception strategy. First, the available slots definition drastically changes. All the limitations imposed by the mission are reduced to bare essentials. The idea is that the AOC can exploit all the slots which are not exploited for other essentials operations for the composition of its plan. As shown in the figure Fig:(5.2), this increase the overall available time for the construction of the avoidance plan.

A second important aspect regards the introduction of new crucial parameters:

- the **time of closest approach** with the secondary. It represents a key point in the conception of the new horizon: the Collision Avoidance Manoeuvre (CAM) will be calibrated with reference to this date.
- the **Warning End date** : t_{WE}. It is the estimated date until which it is necessary to take advantage of the extended slots in order to recover the guidance orbit, once passed the risk. Obviously, we have $TCA < t_{WE}$.

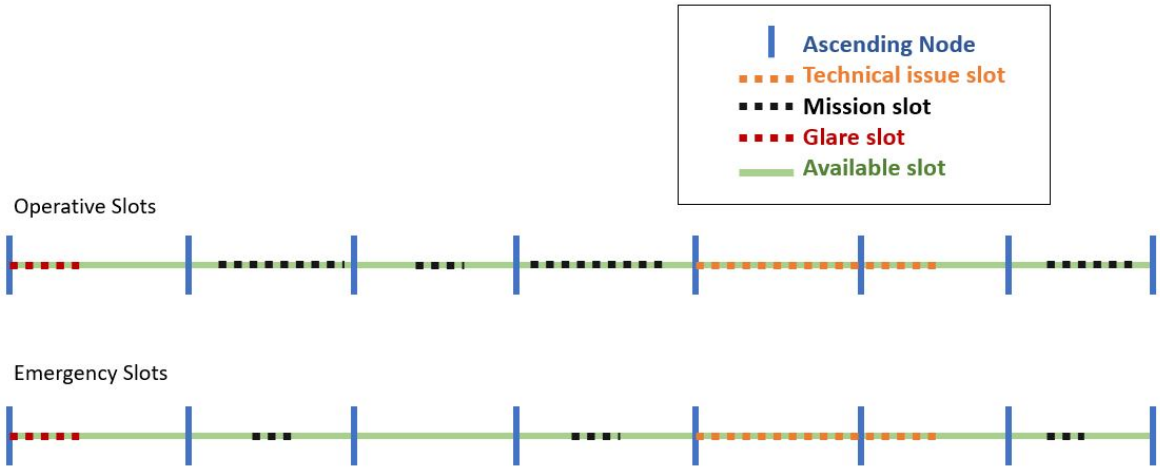

Figure 5.2: Comparison between Operative Horizon and Emergency One

5.1.1.1 Re-entering phase

An important aspect that should be taken into account in the conception of an avoidance collision plane is the $post - t_{CA}$ phase. The avoidance manoeuvre can potentially disturb the mission by determining a deviation of the satellite from its guidance orbit. Once passed the risk of collision, it is then important to proper restore the satellites' trajectory. For this purpose, after computing the manoeuvre plan which allows to avoid the encounter with the secondary, the AOC maintains an "alert configuration" which:

- guarantees a good collision risk treatment.
- slowly reconsiders the restauration of the station keeping mission.

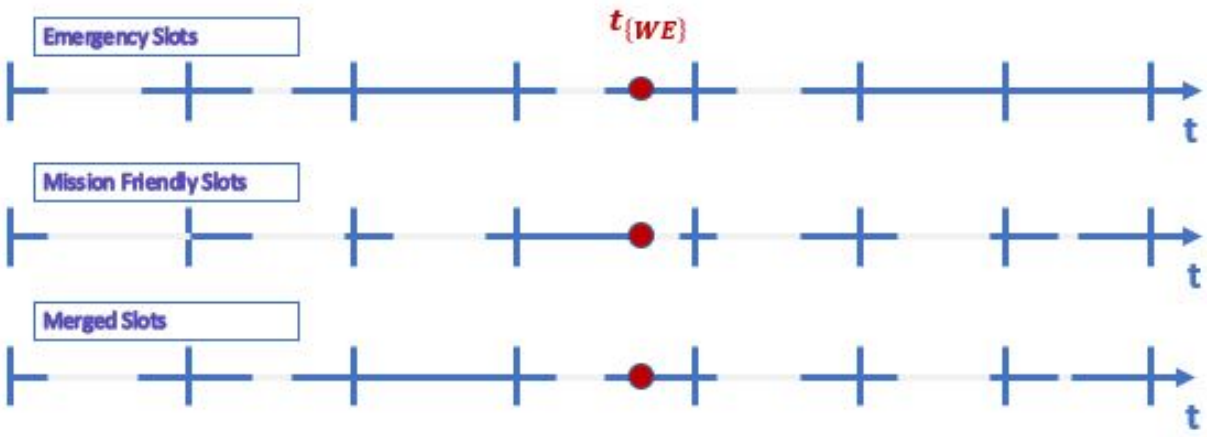

Figure 5.3: Slots merging at the t_{WE}

This twofold nature in the algorithm configuration implies the superposition of the two different modalities of functioning in correspondence of a specific temporal point which is represented by the t_{WE}. As shown in the figure Fig:(5.3), in this phase the AOC treats then a heterogeneous horizon formed by:

- a first window in which the emergency slots are considered. It starts from the activation date up to t_{WE}. It contains both the avoidance plan which covers the part up to the t_{CA} and the computation of the station keeping manoeuvres which are needed for recovering the guidance orbit.

- a second part with the "mission friendly" slots. In this second part the AOC is thought to have recovered the reference orbit, it is then back to the nominal configuration.

5.2 Missions characterisation

The table Tab:(5.2) contains the orbital characterisation of the missions analysed for the simulation, while the table Tab: (5.3) presents the relative temporal horizon configuration. In particular, for each mission it lists:

- the number of orbits in the whole investigation horizon;

- the number of orbits which are frozen;

- the number of semi frozen orbits;

ID	Mission Type	Altitude $[km]$	i °C	LT	Propulsion	Solar Activity
A1	Observation Constellation	470	SSO	10:30	Chemical Electrical	High
A2	Observation Constellation	470	SSO	10:30	Chemical Electrical	Medium
B	Optical Imaging	689	SSO	10:30	Chemical	High
C	Earth Observation	689	10	-	Chemical Mixtes Electrical Mixtes	High
D	Scientific Environment	800	SSO	22:00	Chemical Electrical	High
E	Telecom	1200	88	-	Chemical Electrical	High
F	Altimetry	1336	66	-	Chemical	High

Table 5.2: Analysed Missions Characterisation

ID	Total Horizon	Frozen Orbits	Semi Frozen Orbits
A	11	5	6
B	15	15	0
C	13	5	8
D	14	7	7
E	13	8	5
F	12	7	5

Table 5.3: Missions Horizon Caracterisation

5.3 Towards ASTERIA: Introduction of a Manoeuvre Uncertainty Model in CROCO

The version of CROCO presented in the chapter Ch:(4) does not consider in its analysis the presence of possible station-keeping manoeuvres. It analyses the trajectory of the primary without knowing if some manoeuvre has concurred in its formulation. Nevertheless, they must be taken into account, because, in addition to modify the orbit evolution, they do represent a source of uncertainty that can not be ignored. The literature has investigated the formulation of analytical models for estimating the impact of impulsive manoeuvres in the development of effective methods for orbital uncertainty propagation. For example, Yang [36] compares a method based on State Transition Tensors (STT) with Monte Carlo simulations for developing an analytical uncertainty propagation model for satellite relative motion near J_2-perturbed, elliptic orbits. Also Gonzalo [17] in the

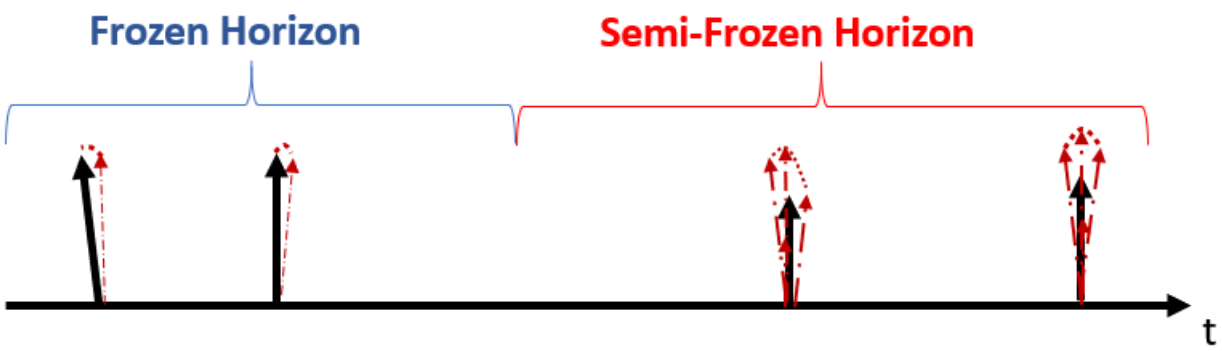

Figure 5.4: Uncertainty on the Predicatble Horizon

construction of a collision avoidance manoeuvre strategy considers in his formulation the presence of uncertainties, by analysing the effect of the lead time between the manoeuvre realisation and the date of the closest approach in the collision analysis, by means of covariances propagations.
These considerations led to the integration in the existing CROCO code of an empirical model that expresses the uncertainty associated to the manoeuvres in function of the time and the manoeuvre type. The uncertainty on a manoeuvre can be visualised by constructing its related uncertainty cone. The figure Fig:(5.4) is an illustration of this concept applied on the manoeuvres contained in a predictable horizon. The region inside the cone represents the spectrum of variability associated to the manoeuvre. Its width increases with the time because of the evident decrease in the prediction accuracy. Both the manoeuvres in the frozen horizon and the ones in the SFH have a proper uncertainty domain. In the first case, it is associated to the inaccuracies in the realisation of the theorical manoeuvre which can impacts both its direction and amplitude. Conversely, the SF cones are significantly wider, because of the additional flexibility given to this temporal segment: the fact that the manoeuvres are adjustable in amplitude influences their uncertainty level. This second source of variation is definitely more significant with reference to the one caused by the realisation inaccuracies. Nevertheless, as the date of their achievement rests frozen, the vertex of each cone is fixed, by guaranteeing to the AOC its predictability handprint. The integration in CROCO's algorithm of model for estimating the uncertainty linked to the changes in amplitude in the Semi Frozen horizon, then, allows to treat more correctly the implementation of the station keeping. The mission considered for this analysis is the mission A2 in table Tab:(5.2) on a temporal horizon of 20 hours , corresponding to 11 orbits. Among them 5 are frozen in time, no wanted ΔV changes can be performed. The remaining 6 orbits are conversely semi frozen and they represent the effective object of the study. The simulation has been conducted several times in order to have a representative spectrum of cases for developing the model. For avoiding misunderstandings, in the following we address with ΔV to the amplitude

of the manoeuvres and with ΔV^* to the variation in the manoeuvres' amplitude in the SF horizon. The procedure here presented concerns the manoeuvres in Δa. However, an analogue analysis for the out-of -plane control has been conducted.
For each manoeuvre planned in the SF horizon, the variation $\Delta V^*_{hyp,real}$ between the initial proposed amplitude value ΔV_{hyp} for the manoeuvres and the effective realised one, ΔV_{real} has been calculated and stored. The data have been then broken down by belonging orbit at the initial activation. The list of $\Delta V^*_{hyp,real}$s allows to calculate its average value $\hat{\Delta} V^*_{hyp,real}$ and the standard deviation $\sigma_{\Delta V}$ for each orbit.

The figures Fig:(5.5,5.6,5.7) show the results of this first phase of the analysis for the different orbits. It can be seen that the distributions follow an evolution path which can be approximated to a gaussian one with an average value and a standard deviation $\sigma_{\Delta V}$ which change with the orbit. The parametrisation of the gaussian distributions for each semi frozen orbit is given in the table Tab:(5.4).

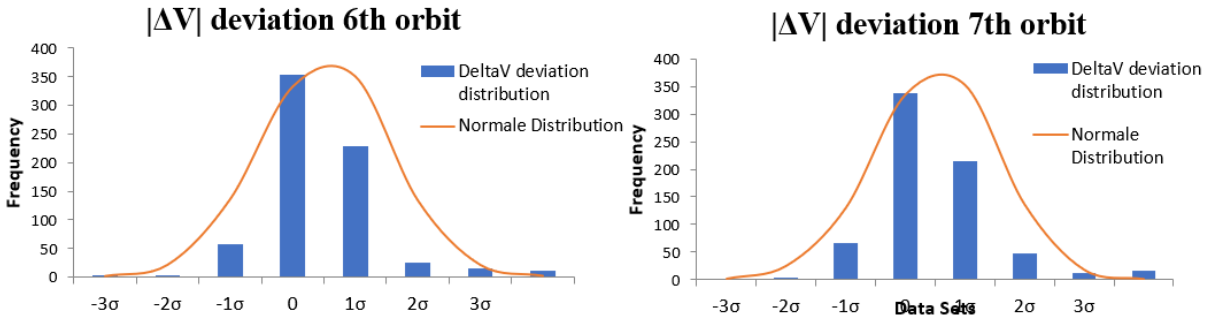

Figure 5.5: ΔV variation in the orbits 6 and 7 of the investigation horizon

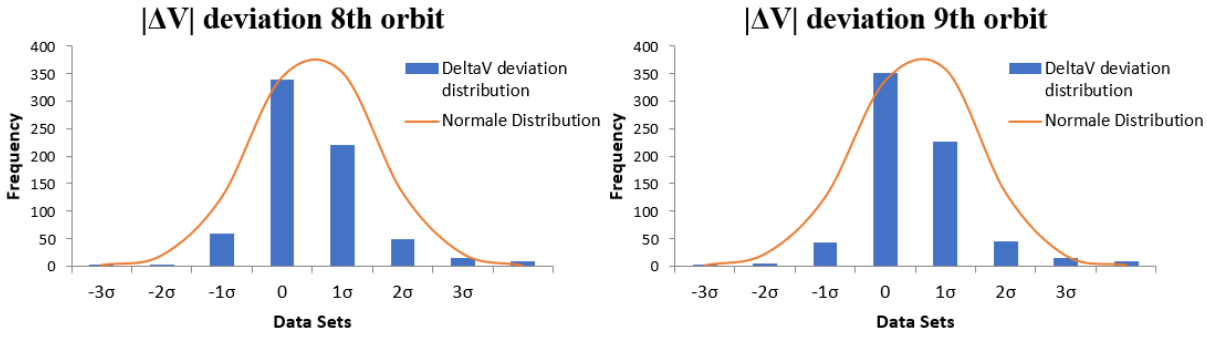

Figure 5.6: ΔV variation in the orbits 8 and 9 of the investigation horizon

Once accepted to model the evolution of the ΔV^* variation along an orbit with a normal distribution, the problem can be reformulated as follows: to express the evolution of the standard deviation across the orbits. The figure Fig:(5.8) show how the $\sigma_{\Delta V}$changes along the investigation horizon.

Finally, thanks to a polynomial regression performed on the collected data, a formulation continous in time have been estrapolated.

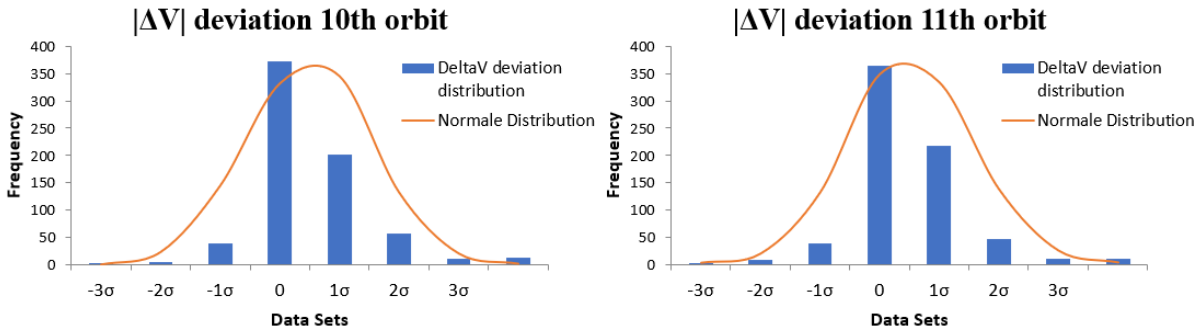

Figure 5.7: ΔV variation in the orbits 10 and 11 of the investigation horizon

Orbit $[n°]$	Mean ΔV^* $[m/s]$	$\sigma_{\Delta V}$ $[m/s]$
6	2.09e-4	1.28e-3
7	3.67e-4	1.96e-3
8	5.88e-4	2.59e-3
9	8.15e-4	3.49e-3
10	12.75e-4	4.61e-3
11	13.84e-4	5.32e-3

Table 5.4: Gaussian distribution model for different orbits

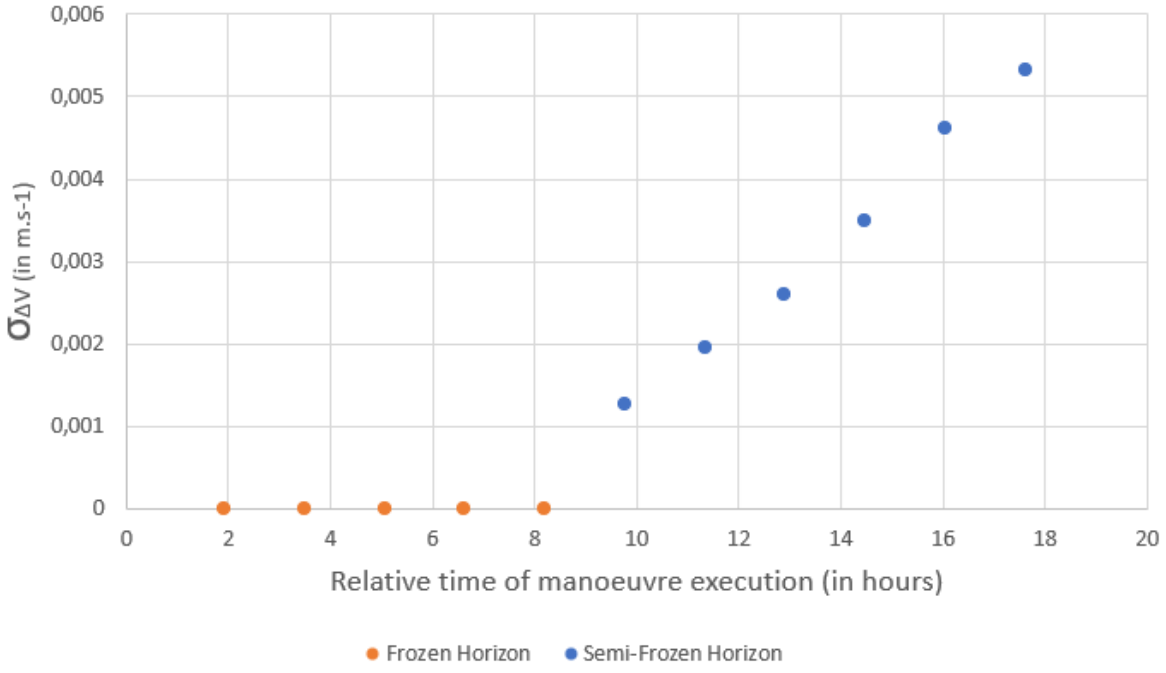

Figure 5.8: Evolution of the standard deviation across the orbits

The equations Eq:(5.1, 5.2) express the mathematical formulation of the resulting models. They give the standard deviation in function of time, respectively in the case of a tangential manoeuvre and a out-of-plane one.

$$\sigma_{\Delta V_T} = -1,36310^{-17}(t_{man} - t_{act})^3 + 3,110^{-12}(t_{man} - t_{act})^2 - 5,64510^{-8}(t_{man} - t_{act}) \quad (5.1)$$

$$\sigma_{\Delta V_W} = 7,91510^{-8}(t_{man} - t_{act}) - 0,002 \quad (5.2)$$

where:

- $\sigma_{\Delta V}$, it's ΔV the standard deviation
- t_{man} is the manoeuvre date
- t_{act} is the OD date

It is not the direction in itself that impacts the uncertainty but the influence that the environment has on one manoeuvre type rather than the other one. The strong effects that the solar activity together with the atmospheric drag have on the ΔT decreased its predictability.
For including the manoeuvres into its computation, the CROCO algorithms, during the covariance propagation of the primary, breaks whenever it encounters a manoeuvre. It corrects the covariance matrix with the standard deviation associated to the manoeuvres and then proceeds with the propagation.

5.4 Towards ASTERIA: introduction of the multi-orbit call

In comparison to the AOC's one, CROCO's calculation is time demanding: the algorithm not only has to treat with a significant amount of input data, but all the propagations are numerical. It implies that the overall computational needed by ASTERIA is incremented. This fact, besides reducing the algorithm performances, can potentially have an even more severe consequence.
In its operative life, the satellite is demanded to realise a wide spectrum of activities, while covering its orbit. Obviously, each operation is characterised by a specific level of priority. It implies that potentially the AOC's calculation is delayed allowing the complete execution of more crucial operations. The situation becomes particularly annoying if the total needed time overcomes the orbital period. Even if this represents a very unlike case, it deserves to be taken into account for preventing an overrunning and eventually a breakdown.

The strategy implemented for solving this potential problem is the introduction of a **Multi-Orbit Call System**: the autonomous control is not called at each ascending node, but only when required.

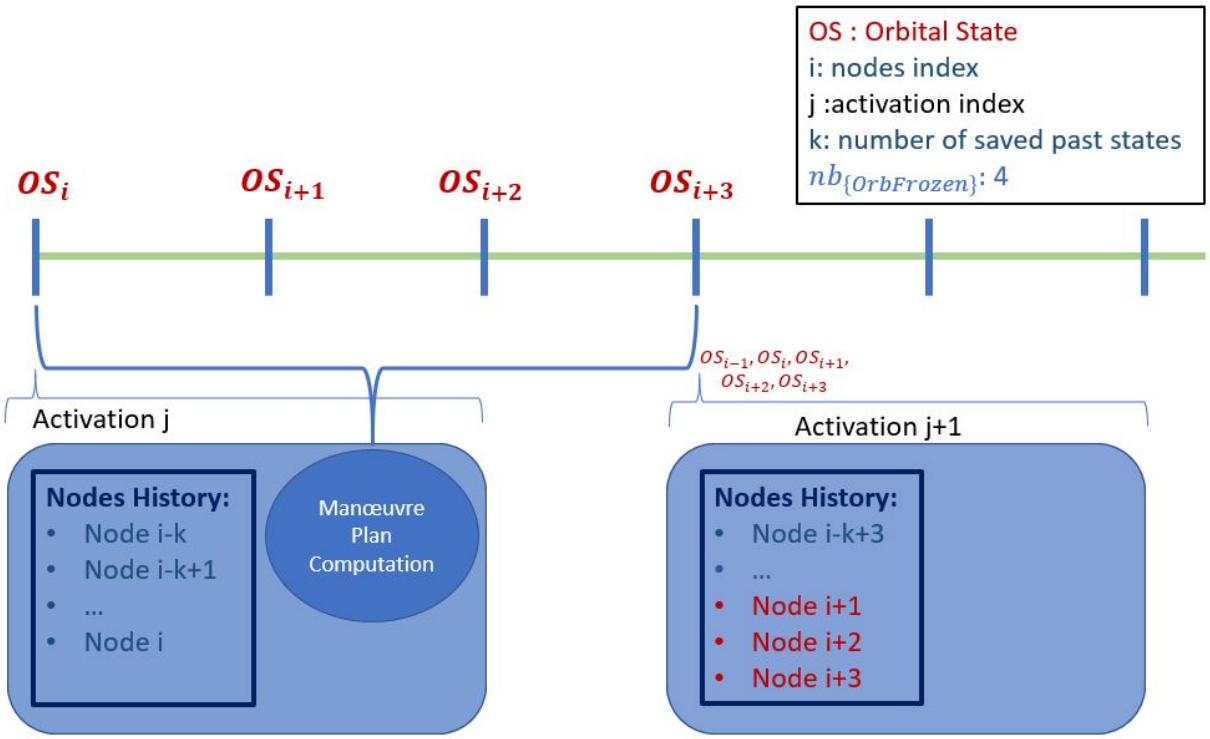

Figure 5.9: Multi-Orbit Call System

Called n_{FH} the number of orbits contained in the frozen horizon of the mission, at each activation the satellite gives to the AOC a list with the information of the orbital states of the last n_{FH}[1] ascending nodes. The controller compares the input list with the current orbital state and then estimates the number of orbit passed since the last activation n_{PAST} and it is then capable to use the provided information as needed for filling the eventually missed information.

The concept is illustrated in the schema Fig:(5.9).

[1]The list length has been set equal to the number of the frozen orbits. It does not make sense to use a greater number. If n_{PAST}>n_{FH} ; it is reasonable to think that the satellite has encountered a sever problem which compromises the proper functioning of the controller

Chapter 6

OPS-SAT Mission

6.1 Mission Overview

OPS-SAT is a 3 Units not manoeuvrable CubeSat designed by the European Space Operations Centre (ESOC) which is orbiting on a LEO dawn-dusk Orbit since the 17 December 2019. It is the first CubeSat operated directly by the ESA. The aim of the mission is to create a in-orbit laboratory for the realisation of authorized software experiments. The satellite is only $30x10x10cm^3$ but it contains an experimental computer which is 10 times more powerful than anyone else used for ESA's spacecraft. Indeed, the main aim of the ESOC is to demonstrate that on-boards computers like the one adopted on OPS-SAT can drastically improve the management of mission operations. Moreover, it represents the first platform to integrally implement the operation protocol developed by CCSDS. The Consultative Committee for Space Data Systems (CCSDS) is an international organization responsible for producing recommendations and standards for space data systems based on the collected experience from previous space missions.

Finally, it enters in the ESA's attempt to make space missions more accessible in term of budget but guaranteeing high versatility, flexibility and performant solutions.

6.2 CNES test campaign

The CNES has obtained the authorisation of exploiting the OPS-SAT platform for conducting a series of tests in 2020 [5]. During this period also the operational versions of the AOC and CROCO will be uploaded on board and tested. The first tests campaign will focus on the original independent versions of the two systems. In a second step also the integral version of ASTERIA will be object of validation.

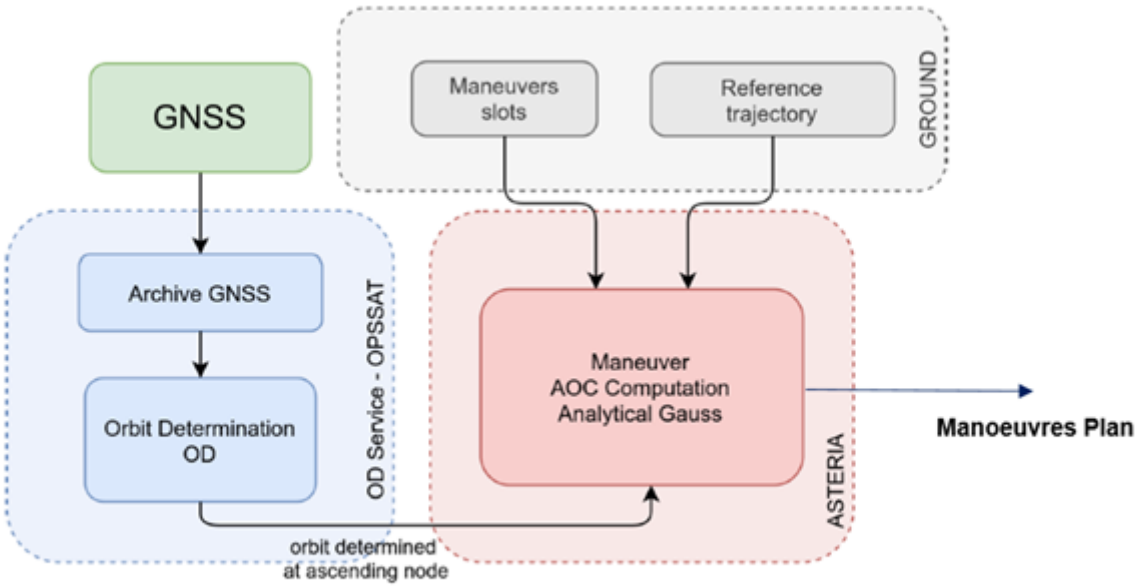

Figure 6.1: AOC OS Application

6.2.1 AOC test

The test campaign on the original version of the AOC system aims to verify the operability of the controller application. In the scheme Fig:(6.1) the main steps are represented:

- By means of a GNSS receiver and a stored history, the satellite performs an orbit determination.
- It uses the orbit restitution for predicting the next ascending node to activate the AOC.
- The AOC, given its inputs (the available temporal windows for performing station keeping manoeuvres and the reference orbit characterisation) , builds the orbital maintenance manoeuvres plan.

It is important to remark that the proposed manoeuvres plan cannot be executed as OPS-SAT has not got a propulsion system. Even if it could represent a significant drawback, the experiment is not conceived for validating the proper functioning of the station keeping, but to test the on-boardability and operability of the autonomous controller.

6.2.2 CROCO test

The CROCO experiment scheme is represented in the figure Fig:(6.2).

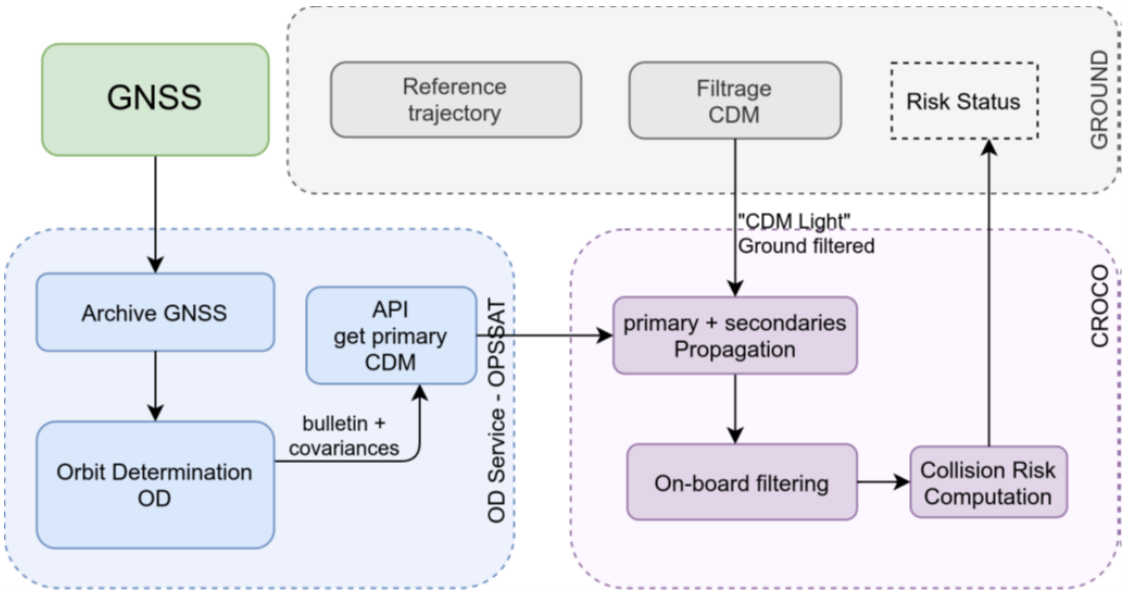

Figure 6.2: CROCO OS Application

- Once again the satellite exploits a GNSS receiver for performing an orbital restitution and determining its current orbital state.
- It then uses this information for the configuration of the primary CDM which contains the state of the satellite as long as its covariance matrix information and the definition of its screening box.
- From the on-ground station it receives the information about the reference orbit and a previously filtered CDM lists with the secondaries (centred on ANGELS).
- It numerically propagates primary and secondaries trajectories and covariances and it identifies the potential collisions.
- It returns the risk status to the on-ground station

6.2.3 ASTERIA test

Once terminated the first campaign on CROCO and the AOC, the next experience will test the integral version of the controller: ASTERIA. These experience have several purposes:

1. to test a proper communication between the two subsystems;
2. to quantify the computational time required;
3. to experiment the multi-orbit call issue;

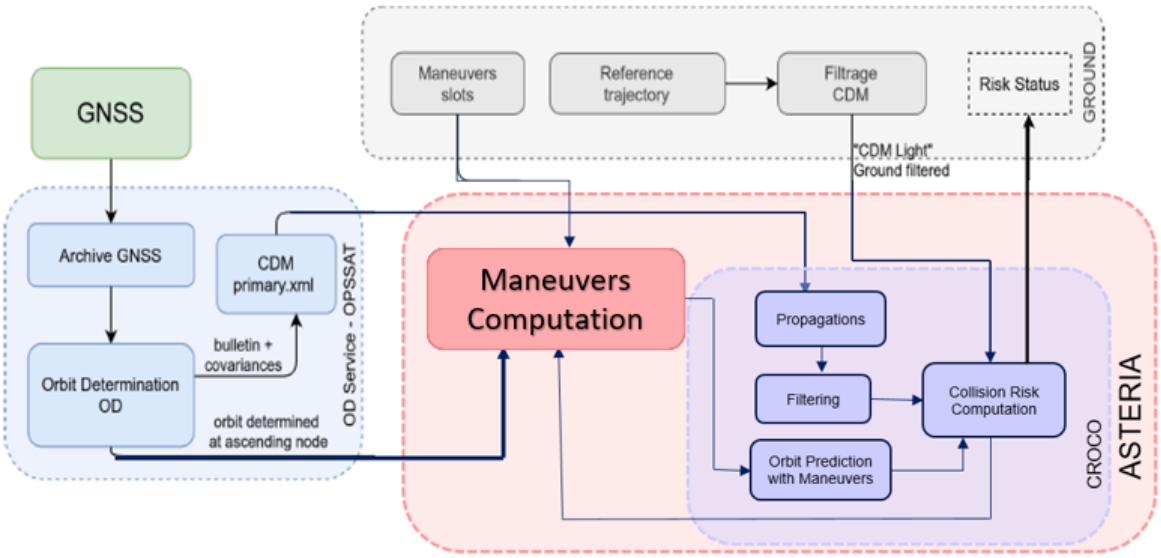

Figure 6.3: ASTERIA OS Application

Chapter 7

Avoidance Plan

This chapter is consecrated to the conception of the Collision Avoidance Manoeuvres plan. The addition of this functionality represents the accomplishment of an important key point in the realisation of ASTERIA.

7.1 Preliminary considerations

The first issue to face in the conception of a collision avoidance plan is the identification of the instruction to give to the controller. Indeed, if on one hand it is evident that the aim is to not produce a collision between the satellite and a secondary object, the translation of this concept in an instruction for the satellite is much less trivial.

7.1.1 CAM determination: typical approaches

The literature on the topic is rich and there are always more experts in the scientific community who show interest on this issue. This is not a surprise considering the parallel increase in the space population: the need of an avoidance manoeuvre which in the last century looked a very unlike situation, is at present a concrete problem to take in consideration for future missions. The papers which treats the design of collision avoidance manoeuvres are then several. Two big branches are typically followed in the conception of the CAM:

- the maximisation of the miss distance between the satellite and the secondary at the t_{ca};
- the minimisation of the collision probability.

It is interesting to note that the achievement of the first goal does not imply the achievement of the second one. Indeed, as demonstrated in [6] the minimum collision probability solution aligns with the smallest principal direction of the covariance ellipsoid. Conversely the maximum ΔV solution lies along the principal direction of the ellipse. The two approaches have pros and cons. In particular, the required δv in the first case is typically higher than the second one, as shown in [17]. Moreover, in the optic of dealing with an always more crowded space, the interest of maximising the relative distance can gradually decreases, because of the possibility of generating a second collision risk. The second strategy, conversely, is characterised by lower δVs. However, the minimisation of the collision probability represents a more complex problem and in consequence it is more time demanding [17]. Despite the conceptual interest that both those solutions have, the approach adopted for this first version of a CAM plan to implement in ASTERIA is different. Indeed, both of the strategies just presented deal with the optimisation of a parameter of interest, while the crucial point is first of all to avoid the collision. The need of a CAM plan in a space mission represents a critical situation to solve as soon as possible. In this sense, in this project, the interest is focused mainly on the quantification of the instruction to give to the satellite to not encounter the secondary. Any optimisation process passes in second floor and is treated in a second time. The strategy adopted in this case concerns the definition of a dynamical **threshold value** beyond which the collision probability is maintained in an acceptable range.
This threshold is represented by a physical relative distance between the estimated positions of the two orbiting objects. The problem characterisation is thus declined in the definition of the two main parameters: the direction and the amplitude of the target gap.

7.1.2 Direction of the imposed deviation

All the three directions $\vec{T}$,$\vec{N}$,$\vec{W}$ present pro and cons:

- a manoeuvre imposed in the **tangential** direction has the advantage of being in general less fuel demanding than an out-of-plane one. Moreover, being an in-plane manoeuvre, its impact on the out-of-plane parameters can be considered negligible at first order. However, the uncertainty cone associated to this direction is wider in comparison to the other ones. Indeed, as already anticipated the environment impacts in particular the parameters which evolves in this direction. The accuracy, which is especially required in this situation leads, in consequence, to discard a $\vec{T}$ solution.

- **normal** direction. A given ΔV_T, in addition to produce a $\Delta\vec{T}$, generates a $\Delta\vec{N}$. The displacements in this last direction are associated to a lower uncertainty and, as generated by a ΔV_T, they keep the advantages listed at the previous point. The drawback is that, in general the ΔV_T required for generating a target $\Delta\vec{N}$ are higher

compared to the ones needed for the equivalent in$\Delta\vec{T}$. In consequence the induced eccentricity deviation can be significant.

- The **out-of-plane** direction incertitude level is relatively low compared to the others. Moreover, a manoeuvre in this direction could be exploited for realising the station keeping and the avoidance at once. However, the out-of-plane manoeuvre is high-fuel demanding and its impact on the in-plane elements can not be neglected

Finally for this thesis work, **the normal direction has been selected**, for the reasons just presented. The analysis of the other directions and in particular the out-of-plane one is left to further studies.

7.1.3 Threshold value

Estimating the value of the normal shift to perform for making a collision risk fall is a complex issue: it depends on several parameters, e.g. the dimensions of the two objects, their covariances matrixes , the t_{CA}, the screening box design. However, it has been possible to indirectly compute it by implementing an iterative method in CROCO. In particular:

1. The collision probability threshold, beyond which the CROCO returns a negative result, is defined.

2. The primary and secondaries propagations provide the information on both the estimated collision probability and the expected normal shift at the t_{CA}, $\bar{\Delta}N_{mes}$. The direction of the shift command is selected (N_+, N_-).

3. The propagation is repeated iteratively, by adding at each iteration a normal shift offset to the $\bar{\Delta}N_{mes}$ in the selected direction up to when the collision probability estimation at the t_{CA} gives a value which fulfils the point 1.

4. The value of the normal shift at the t_{CA} at this point $\bar{\Delta}N_{target}$ expresses the gap that must be guarantee between the two objects.

5. The minimal normal shift command to provide is then:

$$\bar{\Delta}N_{comm} = \bar{\Delta}N_{target} - \bar{\Delta}N_{mes} \tag{7.1}$$

The figure Fig:(7.1) represents a scheme of a situation at the t_{CA} which requires a Collision Avoidance Manoeuvre and the relative normal shifts. It is worth to underline that, as shown in the figure, there are two possible directions for $\bar{\Delta}N_{comm}$. Even if the priority is given to the one of them characterised by a lower amplitude, the existence of the second one represents an alternative that can be exploited in particular cases: for example when the first direction generates a second collision risk.

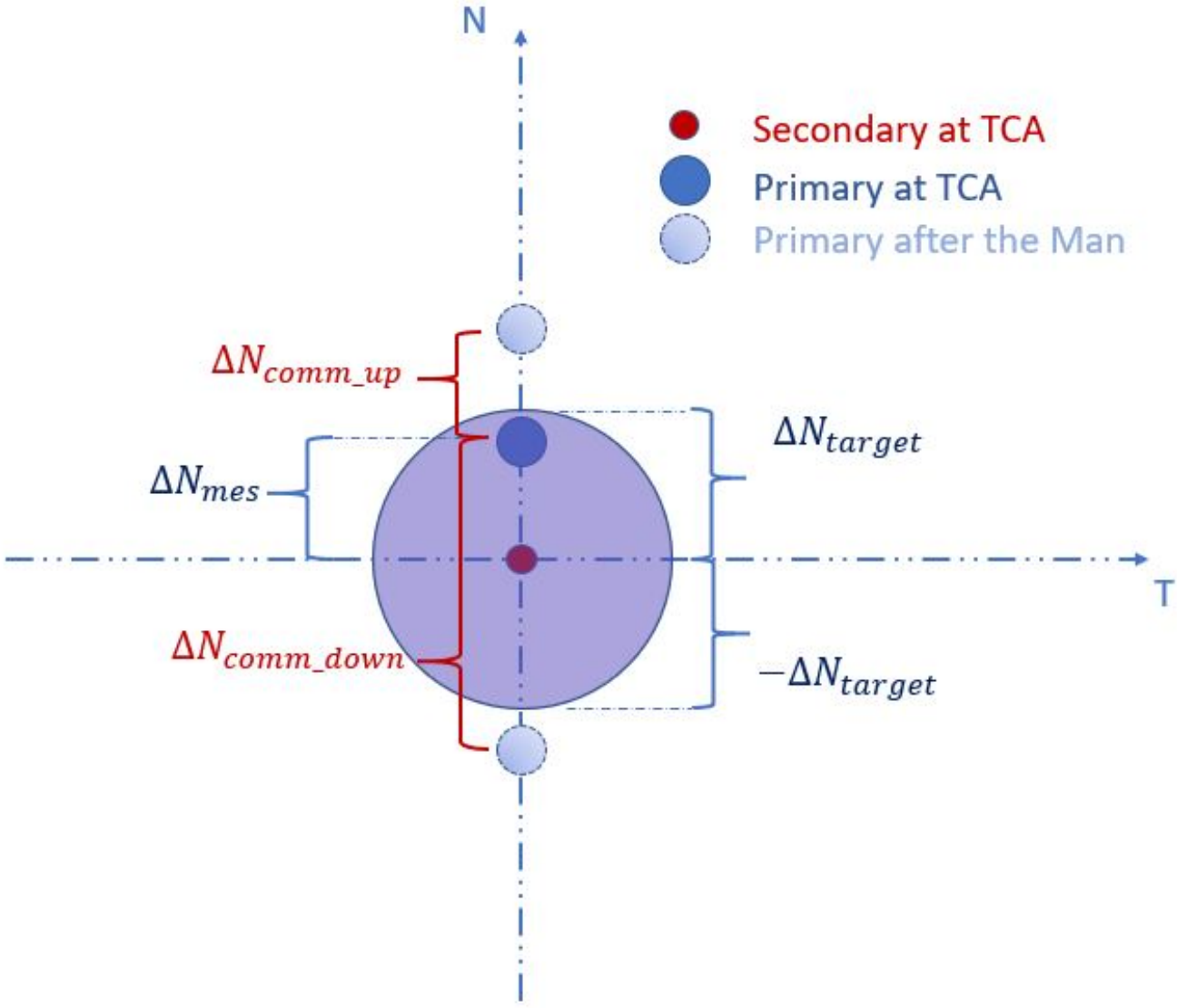

Figure 7.1: Normal Shift at the TCA

7.2 Computation of the manoeuvre for a target $\hat{\Delta}N$

In this section the mathematical formulation at the root of the problem is presented. In particular, the attention is focused on the derivation of the relation between a given manoeuvre performed at the manoeuvre date t_{CAM} and the obtained normal shift with reference to the guidance orbit at the t_{CA}. Before entering the details of this topic, it is important to spend some words in the definition of the several ΔNs. To avoid misunderstandings the following notation is adopted: the apex " $\hat{}$ " is referred to the guidance orbit. Thus, with the symbol $\hat{\Delta}N$ we indicate a normal gap between the satellite and the guiding orbit. Conversely, for referring to the distances with the secondary involved in the collision, we used the symbol " $\bar{}$ "($\bar{\Delta}N$). For further clarification, the reader can refer to the following table, where the used ΔNs are listed and described.

ID	Description
$\hat{\Delta}N_{mes}(\ t_{CA})$	is the normal shift between the satellite and its theorical position on the reference orbit. It is calculated at the t_{CA} if no avoidance manoeuvre is performed .
$\hat{\Delta}N_{real}(\ t_{CA})$	is the normal deviation with reference to the guidance orbit which results at the t_{CA} after realisation of the manoeuvre plan.
$\bar{\Delta}N_{mes}(\ t_{CA})$	is the estimated normal distance at the t_{CA} between the primary and the secondary if no manoeuvre is done
$\bar{\Delta}N_{target}(\ t_{CA})$	is the minimum distance to achieve between the two objects for exiting the dangerous situation.
$\bar{\Delta}N_{real}(\ t_{CA})$	is the normal gap between the two objects at the t_{CA} if the manoeuvres are realised
$\bar{\Delta}N_{comm}(\ t_{CA})$	is the instruction to give to the satellite for guaranteeing to achieve $\bar{\Delta}N_{target}(t_{CA})$. It is positive in the positive direction of the $\vec{N}$ axis

Table 7.1: Radial Gaps definition

With these premisses, according to [17], the deviation in position between the satellite and its associated position on the reference orbit can be expressed in function of the orbital elements by means of the following equation:

$$\delta\vec{r}(t_{CA}) = G_{r\zeta} \quad \delta\vec{\zeta}(t_{CA}) \tag{7.2}$$

where:

$$\delta\vec{\zeta} = [\delta a \quad \delta e_x \quad \delta e_y \quad \delta i \quad \delta\Omega \quad \delta\alpha]^T \tag{7.3}$$

$$\delta\vec{r} = [\delta T \quad \delta\hat{N} \quad \delta W] \tag{7.4}$$

$$G_{r,\zeta} = \begin{bmatrix} 0 & 2sin\alpha & -2cosa\alpha & 0 & cos(i) & 1 \\ -1 & acos\alpha & asin\alpha & 0 & 0 & 0 \\ 0 & 0 & 0 & asinalpha & -cos\alpha sini & 0 \end{bmatrix}$$

is the matrix form of the Gauss planetary equations [17]. What we are interesting in is, in particular, the variation in the normal position $\hat{\Delta}N(t_{CA})$. Considering dealing with impulsive manoeuvres it can be expressed as:

$$\hat{\Delta}N(t_{CA}) = -\Delta a(t_{CA}) + a(\Delta e_x(t_{CA}) * cos\alpha(t_{CA}) + \Delta e_y(t_{CA}) * sin\alpha(t_{CA})) \tag{7.5}$$

As already presented in the chapter Ch:(3), the evolution of the SMA is considered linear, while the eccentricity deviation can be expressed by means of the equations Eq:(2.122.13). The Eq:(7.5), expressed in function of the orbital state at the time where the CAM is

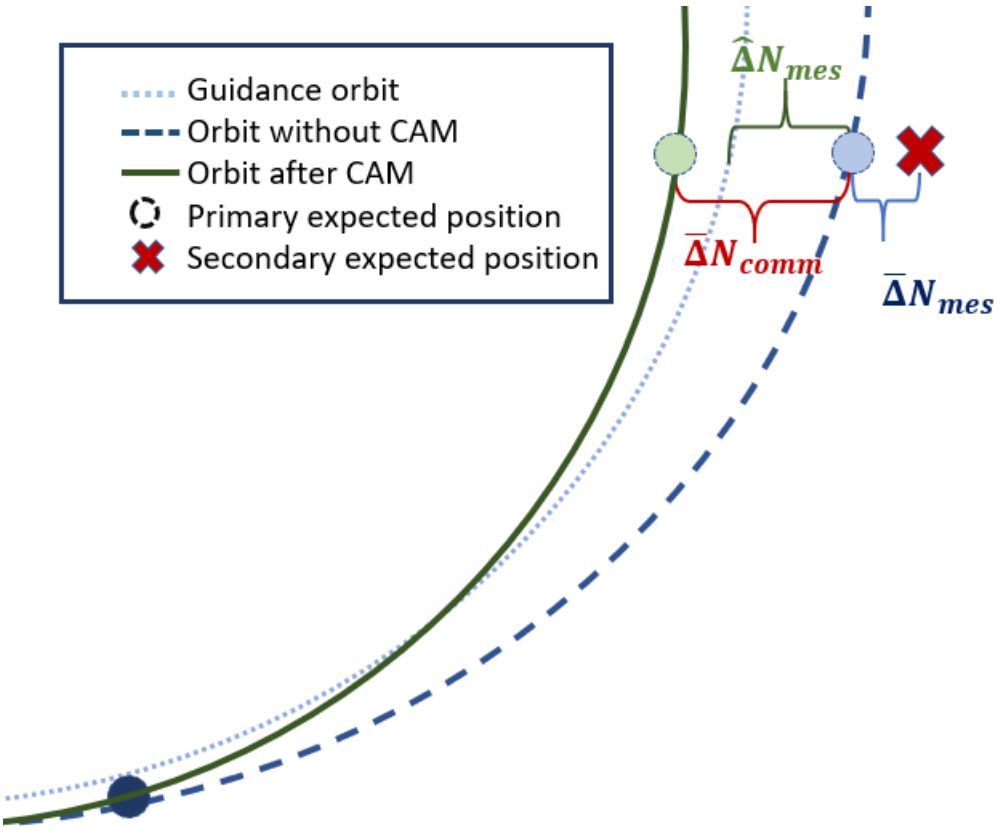

Figure 7.2: Avoidance Scheme

performed, is then :

$$\begin{aligned}\hat{\Delta}N(t_{CA}) = -\Delta a(t_{CAM}) - \frac{\Delta\ddot{\alpha}(t_{CAM}) * \Delta t}{k_{\alpha a}} \frac{\Delta V_T * 2 * a}{V} + \\ a((\Delta ex(t_{CAM}) + \Delta\dot{e_x}(t_{CAM}) * \Delta t \frac{\Delta V_T * 2}{V} cos\alpha(t_{CAM})) * cos\alpha(t_{CA}) + \\ (\Delta ey(t_{CAM}) + \Delta\dot{e_y}(t_{CAM}) * \Delta t \frac{\Delta V_T * 2}{V} sin\alpha(t_{CAM})) * sin\alpha(t_{CA}))\end{aligned} \tag{7.6}$$

with $\Delta t = t_{CA} - t_{CAM}$.

The Eq:(7.6) expresses the relation between a manoeuvre in ΔV_T given at the t_{CAM} and the resulting deviation $\hat{\Delta}N$. In consequence, once computed the $\bar{\Delta}N_{comm}$ as described in the last paragraph, it can be linked to the $\hat{\Delta}N$ thanks to following expression:

$$\bar{\Delta}N_{comm} = \hat{\Delta}N_{real}(t_{CA}) - \hat{\Delta}N_{mes}(t_{CA}) \tag{7.7}$$

7.3 Collision Avoidance Manoeuvre Date Selection

Once determined the instruction in terms of ΔN to give to the primary for accomplishing the avoidance, it still rests an important parameter to set: the manoeuvre date. The constraints in the definition of the problem are the following:

- $\bar{\Delta}N_{real} >= \bar{\Delta}N_{target}$. It represents the crucial constraint to satisfy in order to overcome the risk. This condition has the priority to all the other parallel objectives.
- $\Delta V_T <= \Delta V_{MAX}$. We have already spoken about the limitations on the ΔV imposed by the propulsion system. The single manoeuvre can not overcome this limitation. Nevertheless, if the avoidance requires a greater ΔV, it can be possible to split it across several slots.
- the date of the manoeuvre must fall within one available slot

Once listed the requirements to fulfil, the parameters which can be calibrated in order to accomplish the avoidance must be identified. Each of them plays a role in the definition of the CAM. We have:

1. the position on the orbit α. The argument of latitude at which the manoeuvre is performed impacts the resulting $\hat{\Delta}N$ at the t_{CA}. In particular, for maximising the effects of a given ΔV_T, the manoeuvre should be performed at an α opposite with reference to the one at the date of closest approach.
2. the temporal advance from the t_{CA}. A collision risk can be detected with such an advance that allows to perform the CAM at different temporal slots before the potential collision. The question is consequently which one should be chosen. On one hand, a earlier reaction allows to earlier exit the dangerous situation. On the other one, a reaction closer to the t_{CA} can be better calibrated thanks to a better knowledge of the orbits of the two objects. Moreover, an early reaction can result in an amplification of the deviation from the guidance orbit.
3. the direction of the $\bar{\Delta}N$. As previously anticipated the given ΔV_T can generate a normal shift in both N_+or N_-. In particular; a manoeuvre in SMA_{Up}, by increasing the semi major axis, generates a negative $\hat{\Delta}N$. Conversely a manoeuvre in SMA_{Down} produces a positive $\hat{\Delta}N$. Referring to the figure Fig:(7.1) the first selected direction is the same as the starting $\hat{\Delta}N_{MES}$, e.g. the one which requires a $\hat{\Delta}N_{comm}$ lower in amplitude.
4. the ΔV_T amplitude. A higher ΔV_T results in a normal shift higher in amplitude at the t_{CA}, but it implies a stronger eccentricity correction and a stronger deviation from the nominal orbit.
5. the number of manoeuvres. It is possible to split the total ΔV_T needed for performing the avoidance plan along several slots. This can be particularly useful in case of an electric propulsion system, when in any case the ΔV can potentially be distributed because of the limitations of a low thrust system. Moreover the fact of splitting the manoeuvre could represent a solution of the point 2 by both reacting as soon as possible to the risk and at the same time by giving the possibility of updating the remaining ΔVs in itinere.

Several simulation cases have been conducted with a different calibration of the previously listed parameters. The common point is the fulfilment of the requirements and the limitation of the degradation of the mission, by reducing the impact on the tangential direction. The results are presented in the following paragraph. The mission considered for this analysis is the A2 in the table Tab:(5.2).

7.4 Avoidance plan simulation

The interest of this analysis is to simulate an avoidance realisation and to analyse the effects of the CAM plan on the station keeping. This study focalises on the mission A2, by reproducing different avoidance strategies and comparing the results. For reproducing a real situation, the canonical slots used for the previous simulations have been changed to an emergency version. Obviously, it means that there are more available slots for performing the manoeuvres.

The mission is analysed in a temporal window of the 10 days. At the 7th day a secondary object is supposed to enter the security sphere of the satellite. It is then necessary to prevently react for avoiding the collision. Different target values for the $\bar{\Delta}N_{target}$ in N_+ and N_- have been defined.
Five different strategies are proposed:

1. single manoeuvre: the AOC realises a single CAM as close as possible to the t_{CA}.
2. split manoeuvre: the AOC equally splits the manoeuvre on all the available slots.
3. double "low-high" manoeuvre: the AOC splits the manoeuvre in two not equal parts, respectively in the 30 and 70 % of the total needed ΔV.
4. double "high-low" manoeuvre: the AOC splits the manoeuvre in two not equal parts, respectively in the 70 and 30 % of the total needed ΔV.
5. double "half-half" manoeuvre: the AOC splits the manoeuvre in two equal parts.

Apart from the second case, the choice of the slots is slightly optimised: if possible the AOC choices the slot/s which implies the lowest effects on the ΔT. In particular the priority is given to the slot which minimise the following function:

$$\delta e^*_{MAN} * \Delta T^*(t_{CA}) \tag{7.8}$$

where δe^*_{MAN} is the correction in eccentricity caused by the manoeuvre. The apex " $.^*$ " simply indicates that the two parameters have been normalised with a proper reference value.

The main interest of this comparison is to analyse how the manoeuvre configuration can play on its realisation and on the induced effects on the satellite orbital deviation. In particular we are interested in the following parameters:

- the argument of latitude of the manoeuvre point: α_{CAM}. As already anticipated, the optimal AOL is opposed to the one at the t_{CA}. Unfortunately, even if in an emergency situation, the wanted α could potentially not be available for realising the manoeuvre. The simulation of the split manoeuvre aims to reproduce a situation in which not all the available slots allow to have $\alpha_{CAM} = \alpha_{opt}$. In particular, in this case the manoeuvre is split in six parts. Among them, 3 are performed at an AOL which is not the optimal one.

- the temporal advance from the t_{CA} and the thrust repartition. The interest of the three double-manoeuvre strategies is to compare how the thrust repartition impacts the induced effects on the orbit.

In the table Tab:(7.2) the total needed ΔV for the different values of $\bar{\Delta}N_{comm}$ is given. In particular the first column gives the ΔV needed when it is possible to realise the manoeuvre in correspondence of the optimal AOL . The second one refers to the split simulation, when three among the six manoeuvres are forced to a different α_{CAM}. What

$\bar{\Delta}N[m]$	$\Delta V_{optimal}[m/s]$	$DeltaV_{splitted}[m/s]$
50	- 0.014	-0.021
100	-0.028	-0.042
200	- 0.056	-0.084
300	-0.084	-0.126
400	-0.112	-0.168
500	-0.140	- 0.210
-50	0.014	0.021
-100	0.028	0.042
-200	0.056	0.084
-300	0.084	0.126
-400	0.112	0.168
-500	0.140	0.210

Table 7.2: ΔV Needed for Different Normal Shifts

emerges is that as expected the fact of can not always exploit the optimal orbital position determines an over consumption. The reader could have notice that the results in ΔV are linear with the ΔN evolution. This is not surprising if considering that the t_{CA}, the $\alpha_{man}s$ are the very same from on case to the other one. In this situation we then have $\hat{\Delta}N \propto \Delta V_T$. The figure Fig:(7.3) represents the tangential shift induced by the different strategies at the t_{CA}. In particular it wants to compare the situations in which it is possible to perform the manoeuvre(s) at the optimal AOL, in order to compare the time influence on the induced ΔT. The linear evolution is again due to the fact, once fixed the argument of latitude and the date of the t_{CA} the ΔT depends only on the ΔV_T given in correspondence of the manoeuvre. What emerges from these results is that the thrust time does play an important role on the final ΔT. In particular, realising the manoeuvre as close as possible

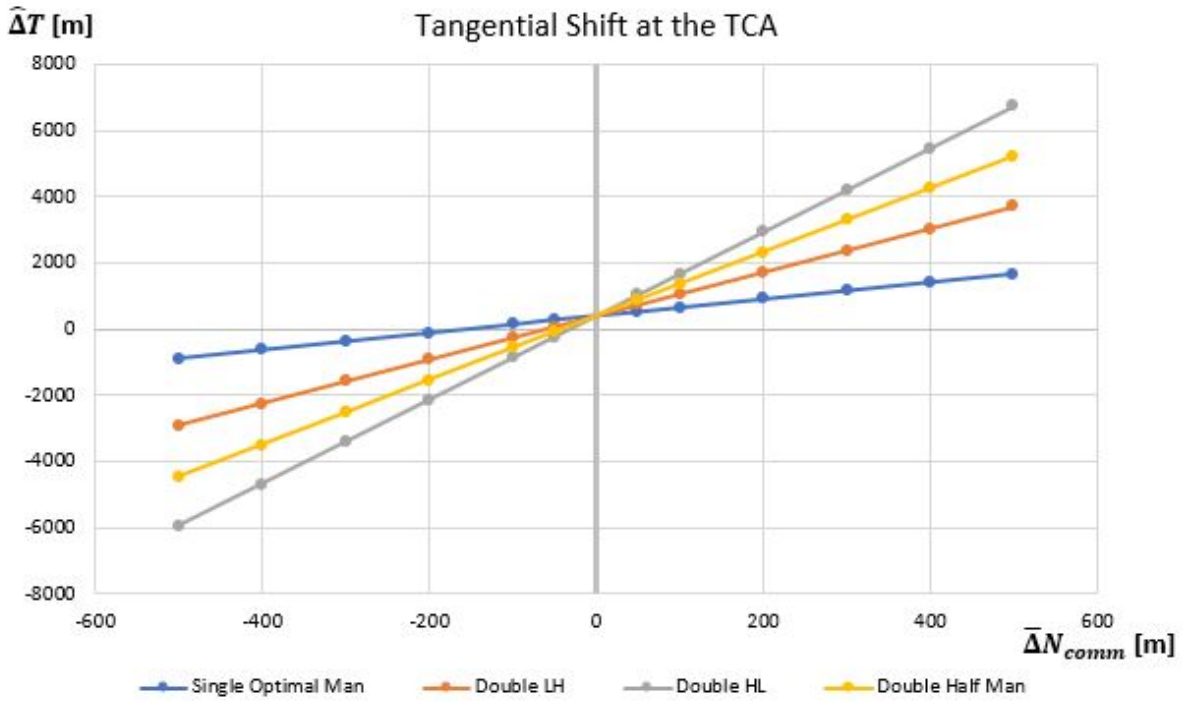

Figure 7.3: Induced ΔT for Different Normal Shifts

to the t_{CA} results in a lower ΔT. In these terms a single optimal manoeuvre is preferrable to a split one which implies an increment in the tangential deviation. If it is not possible to perform a single manoeuvre because of, for example, propulsive limitations, the best strategy to adopt is to sort the manoeuvres for increasing ΔV.

7.5 Reintegration of the mission

Another important point to consider in the implementation of a collision avoidance plan is how to recover the nominal configuration once the risk is passed. This last part of this chapter focuses on this issue. The aim is to give an order of magnitude to the recovering time after the t_{CA}. It is particularly important for the construction of the merged horizon presented in the chapter Ch:(5.1.1.1). The missions analysed are the same which have been studied in the previous section.
First, it must be defined what "recover" means. The approach chosen in this simulation is the following: the recovering time is represented by the temporal interval between the t_{ca} and the instant where the satellite renters the virtual box. The procedure goes as follows:

1. After the calculation of the CAM, the AOC waits for the risk to be passed before trying to restore the guidance orbit.

2. Passed this time the AOC realises the manoeuvre which allows the satellite to re-entering the nominal SK conditions.

3. The time needed for re-entering the virtual box is calculated.

In the analysis, two different threshold for the dimensioning of the virtual box have been considered. The time lapses associated to their recoveries are respectively defined as: Δt_{rec1} and Δt_{rec2}. The table Tab:(7.3) shows the obtained results. In the table the symbol "-" indicates that the CAM does not comport the exit of the virtual box, so in these cases the recovering time is not defined.

$\bar{\Delta}N_{comm}[m]$	Single	Double HL	Double LH	Double Half	Split
50	Δt_{rec1} :- Δt_{rec2} :-	Δt_{rec1} :- Δt_{rec2} :-	Δt_{rec1} :- Δt_{rec2} :-	Δt_{rec1} :- Δt_{rec2} :-	Δt_{rec1} :1.2 Δt_{rec2} :-
100	Δt_{rec1} :- Δt_{rec2} :-	Δt_{rec1} :0.8 Δt_{rec2} :-	Δt_{rec1} :- Δt_{rec2} :-	Δt_{rec1} :- Δt_{rec2} :-	Δt_{rec1} :2.4 Δt_{rec2} :-
200	Δt_{rec1} :- Δt_{rec2} :-	Δt_{rec1} :2.3 Δt_{rec2} :-	Δt_{rec1} :1.6 Δt_{rec2} :-	Δt_{rec1} :3.4 Δt_{rec2} :-	Δt_{rec1} :11.8 Δt_{rec2} :4.8
300	Δt_{rec1} :- Δt_{rec2} :-	Δt_{rec1} :7.1 Δt_{rec2} :0.3	Δt_{rec1} :5.12 Δt_{rec2} :-	Δt_{rec1} :6.24 Δt_{rec2} :-	Δt_{rec1} :19.1 Δt_{rec2} :14.3
400	Δt_{rec1} :- Δt_{rec2} :-	Δt_{rec1} :9.6 Δt_{rec2} :0.6	Δt_{rec1} :8.64 Δt_{rec2} :0.2	Δt_{rec1} :9.7 Δt_{rec2} :1.2	Δt_{rec1} :26.4 Δt_{rec2} :19.3
500	Δt_{rec1} :0.4 Δt_{rec2} :-	Δt_{rec1} :16.4 Δt_{rec2} :6.7	Δt_{rec1} :11.5 Δt_{rec2} :2.3	Δt_{rec1} :16.5 Δt_{rec2} :5.3	Δt_{rec1} :37.8 Δt_{rec2} :26.7

Table 7.3: Orbital Recovering Time [h]

7.6 Considerations and perspectives

This chapter have covered some important points in the conception of an emergency plan for avoiding the collision with a secondary object. The strategy followed is based on the identification of a value for the normal shift between the two objects that, once overcome, assures to have an acceptable value for the collision probability. Once identified this threshold the starting AOC algorithm has been upgraded by adding the necessary tools for computing an avoidance plan which allows to fulfil the requirements. Unfortunately for lack of time it would not have been possible to deeper analyse the topic. For further developments it would be interesting to:

- expand the study by considering a different strategy which exploits the out-of-plane direction instead of the in-plane one. It would be interesting, in fact to evaluate the possibility of realising a CAM in ΔV_W . Considering the relatively high cost of an

out-of-plane manoeuvre plan, this solution could gain interest if coupled with the station keeping mission.

- actuate an optimisation process. The code realised looks mainly to the fulfilment of the constraint and the limitations of the side effects of the CAM realisation. It would be fine to refine the analysis by including a more structured optimisation process.
- consider a different strategy for the recovery phase. The recovery segment presented in this chapter is conceived for restoring the SK nominal conditions as soon as possible by basically counteracting the deviation induced by the CAM. An alternative could be represented by the possibility of creating a transitional phase which gradually restores the nominal condition but that can be nevertheless exploited for realising (at least partially) the mission. This solution can be very interesting considering mission as the D one, which shows relatively long recovering time.
- consider the possibility of treating more than one secondary. As previously said, the increment in the space population together with the refinement of space objects detection, result in a potentially more frequent need of a CAM computation. In this optic, it would be unwise to consider just one secondary in this analysis. It would be significantly preferrable to build a manoeuvre plan which consider several collision risks at once.

Chapter 8

Conclusions and Perspectives

The fundamentals of the autonomous orbital controller (AOC) and the collision risk on-board calculation system (CROCO) developed by CNES have been presented. The two systems have been merged in ASTERIA: an integral version which guarantees the station keeping, identifies the collision risk thanks to a probabilistic computation and finally builds a collision avoidance manoeuvres plan in case of detection of a collision risk. Several aspects have been considered in the realisation of ASTERIA. The original core of the AOC has been expanded for welcoming CROCO. This process includes the integration of a new model for estimating the uncertainty linked to the manoeuvres contained in the plan proposed by the AOC. Thanks to this new model the collision probability calculation can integrate the station keeping in its analysis for the identification of the future encounters with the satellite's neighbourhood. In a second time the strategy for the conception of a collision avoidance manoeuvres plan has been presented. The avoidance is achieved by means of the guarantee of a minimal normal distance between the satellite and the secondary under analysis. The plan has been conceived for completely satisfy the normal shift requirements. In parallel a recovering guidance orbit strategy has been introduced with the aim of giving an order of magnitude to the time needed for restore the station keeping nominal conditions. The single subsystems together with the integral version ASTERIA are planned to be tested within the OPS-SAT mission with the aim of ulteriorly test the on-boardability of the new control system.

In future it would be interesting to develop this analysis by focusing on the following points:

- for the uncertainty manoeuvres model, it can be interesting to expand the current model by considering not only the variation in amplitude of the manoeuvres in the semi-frozen horizon but also the changes in direction. It would represent a

refinement of the model and the CROCO's computation would benefit of it. Moreover the method adopted so far is empirical. It could be interesting to evaluate the possibility of integrating an analytical method, by inspiring to the ones proposed in the literature for obtaining a greater accuracy in the formulation of the problem.

- Concerning the avoidance plan, it would be a good idea to consider different strategies and to consider the possibility of optimising the process. In particular the out-of -plane solution can be analysed and then compared to the one proposed in this work. Moreover, the selection of the manoeuvre date and of its amplitude can be optimised. Nevertheless, it is important to always keep in mind that the resort to a CAM plan represents an emergency situation. Finally, it can be wise to extend the collision avoidance computation to a multi-secondary analysis, by admitting to have several collision risks at once.

Bibliography

[1] V. D. A. "Fundamentals of Astrodynamics and Applications." In: *Space Technology Library* 1.4, 8.2, 8.3, 10.4 (1997).

[2] *Air Force Space Command to discontinue space surveillance system*. 2013.

[3] "Anti-satellite Tests in Space - The Case of China." In: *Secure World Foundation:Technical report* (2014).

[4] H. Bernstein and C. C. Chao. "Onboard stationkeeping of geosynchronous satellites using a global positiong system receiver." In: *Journal of guidance, control and dynamics* (1994), p. 17.

[5] A. D. Bolivar. "Development and operation of on-board applications of the ESA OPSSAT satellite." In: *Technical report* (2020).

[6] C. Bombardelli and J. Hernando-Ayuso. "Optimal Impulsive Collision Avoidance in Low Earth Orbit." In: *JOURNAL OF GUIDANCE,CONTROL,AND DYNAMICS* 38.2 (February 2015).

[7] I. Cavallari. *Predictive Autonomous Orbit Control:Integration of a New Maneuver Type*. Milano, Italy: POLITECNICO DI MILANO, 2019.

[8] K. Chan. "SPACECRAFT COLLISION PROBABILITY FOR LONG-TERM ENCOUNTERS." In: (2020).

[9] C. C. G. Chao. *Applied Orbit Perturbation and Maintenance*. Aerospace Press, 2018.

[10] S. D'Amico, G. Radice, and S. D. Florio. "Precise autonomous orbit control in low earth orbit." In: *Astrodynamics Specialist Conference* (2012).

[11] ESA. *Scanning and observing*. 2018.

[12] ESA. *OPS-SAT Mission*. 2019.

[13] ESA. *Space Surveillance and Tracking*. 2019.

[14] ESA. *Atomic Time*. February 2011.

[15] ESA. *Space Debris by the numbers*. February 2020.

[16] ESA. *Space Environment Statistics*. October 2020.

[17] J. G. Gomez, C. Colombo, and P. D. Lizia. *Analysis and Design of Collision Avoidance Maneuvers for Passive De-Orbiting Missions*. Snowbird, UT, USA, 2018.

[18] D. C. Harrison and J. C. Chow. *The Space-Based Visible Sensor*. 2017.

[19] F. Letizia and C. Colombo. "CONTINUITY EQUATION APPROACH FOR THE ANALYSIS OF THE COLLISION RISK DUE TO SPACE DEBRIS CLOUDS GENERATED BY A FRAGMENTATION EVENT." In: *Conference Paper* (October 2014).

[20] A. P. A. Maute. "Autonomous orbit control method and system for a geostationary satellite." In: *Technical report* 10 (1992).

[21] A. Morselli. "A high order method for orbital conjunctions analysis." In: *Politecnico di Milano* (2014).

[22] NASA. "Advanced avionics concepts: autonomous spacecraft control." In: *Technical report* (1989).

[23] Nice-Matin. "L'accident improbable : deux satellites entrent en collision dans l'espace." In: *Jean-Pierre Largillet* (2009).

[24] R. Pastel. "Estimating satellite versus debris collision probabilities via the adaptive splitting technique." In: (2011).

[25] R. Patera. "General Method for Calculating Satellite Collision Probability." In: *JOURNAL OF GUIDANCE, CONTROL, AND DYNAMICS* (2001).

[26] E. portal. *ANGELS (Argos Neo on a Generic Economical and Light Satellite)*. 2019.

[27] J. Prezeau. "Creation d'un logiciel de calcul des risques de collision pour une satellite en orbite basse." In: *Technical report* (2020).

[28] R. Serra. "Opérations de proximité en orbite: évaluation du risque de collision et calcul de manoeuvres optimales pour l'évitement et le rendez-vous." In: *INSA* (2015).

[29] A. Silberschatz, H. F. Korth, and S. Sudarshan. *Mécanique Spatiale -tome I*. CNES, Toulouse, France: Cépaduès-Editions, 1995, 5.1, 5.A.1.1, 5.A.1.2, 13.4.1, 13.6.2, 13.6.3, 13.6.4.

[30] N. Standard). "Guidelines and Assessment Procedures for Limiting Orbital Debris." In: *SIGPLAN Not.* 43.10 (August 1995), pp. 227–244.

[31] J. Thomassin, M. Echoard, and G. Azema. "Predictive Autonomous Orbit Control Method For Low Earth Orbit Satellites." In: *Flight Dynamics Department* (2017).

[32] *USSTRATCOM Space Control and Space Surveillance*. October 2020.

[33] J. R. Wertz. "Autonomous Navigation and Autonomous orbit control in planetary orbits as a mean of reducing operations cost." In: (2003).

[34] F. P. Will Donald. "Monte Carlo Method for Collision Probability Calculations using 3D Satellite Models." In: (2017).

[35] G. Xing and S. A. Parvez. "Autonomous orbit control with position and velocity feedback using modern control theory." In: *Technical report* (1997).

[36] Z. Yang and Y. zhng Luo. "Nonlinear Analytical Uncertainty Propagation for Relative Motion near J2-Perturbed, Elliptic Orbits." In: *Journal of Guidance, Control and Dynamics* (2018).

ANNEX I

Annex 1: Inclination evolution under the effect of the perturbations

When considering $\frac{di}{dt}$, it is necessary to consider the three main sources of perturbation: the Moon and the Sun gravitation, the atmospheric drag and the terrestrial tides. The last two sources are usually neglected, as the long period variation of inclination is mainly consequence of a third body (Sun and Moon) effect. However, during periods characterized by a strong solar activity it is not possible to neglect the other two sources without committing signi

cant errors. The inclination evolution under the effect of a three body gravitational potential is expressed by:

$$\frac{di}{dt} = \frac{3}{2}\frac{\mu}{nd^3}\frac{Z}{\sqrt{1-e^2}}(cos\omega(1+4e^2)X - sin\omega(e^2)Y) \tag{I.1}$$

ANNEX II

Annex 2: Lagrange Equations

If only conservative forces due to external perturbations are considered, the equations of variations of the Keplerian elements in terms of the disturbing function, R, can be written in the Lagrangian form:

$$\frac{da}{dt} = \frac{2}{na}\frac{\partial R}{\partial M} \tag{II.1}$$

$$\frac{de}{dt} = \frac{1}{na^2 e}((1-e^2)\frac{\partial R}{\partial M} - \sqrt{1-e^2}\frac{\partial R}{\partial \omega} \tag{II.2}$$

$$\frac{di}{dt} = \frac{1}{na^2 \sin i\sqrt{1-e^2}}(\cos i\frac{\partial R}{\partial \omega} - \frac{\partial R}{\partial \Omega}) \tag{II.3}$$

$$\frac{d\Omega}{dt} = \frac{1}{na^2 \sin i\sqrt{1-e^2}}\frac{\partial R}{\partial i} \tag{II.4}$$

$$\frac{d\omega}{dt} = -\frac{1}{na^2 \sin i\sqrt{1-e^2}}\cos i\frac{\partial R}{\partial i} + \frac{\sqrt{1-e^2}}{na^2 e}\frac{\partial R}{\partial e} \tag{II.5}$$

$$\frac{dM}{dt} = n - \frac{1-e^2}{na^2 e}\frac{\partial R}{\partial e} - \frac{2}{na}\frac{\partial R}{\partial a} \tag{II.6}$$